Disorder perturbed flat bands. II. Search for criticality

Pragya Shukla
Department of Physics, Indian Institute of Technology, Kharagpur 721302, India

(Received 29 June 2018; revised manuscript received 23 October 2018; published 7 November 2018)

We present a common mathematical formulation of the level statistics of a disordered tight-binding lattice, with one or many flat bands in the clean limit, in which system-specific details enter through a single parameter. The formulation, applicable to both single- as well as many-particle flat bands, indicates the possibility of two different types of critical statistics: one in weak disorder regime (below a system-specific disorder strength) and insensitive of the disorder strength, another in strong disorder regime and occurs at specific critical disorder strengths. The single-parametric dependence, however, relates the statistics in the two regimes (notwithstanding different scattering conditions therein). This also helps in revealing an underlying universality of the statistics in weakly disordered flat bands, shared by a wide range of other complex systems irrespective of the origin of their complexity.

DOI: 10.1103/PhysRevB.98.184202

I. INTRODUCTION

A dispersionless band, also referred as a flat band, appears in crystal lattices under subtle interplay of the system conditions. The onset of disorder, say w, may lead to violation of these conditions, lifting the degeneracy of the energy levels and changing the nature of the eigenfunction dynamics. The important role played by these bands, e.g., in magnetic systems, makes it relevant to seek the detailed information about the effect of disorder on their physical properties, e.g., if varying disorder may lead to a localization to delocalization transition and whether its nature is similar to other disorder driven transitions.

Previous numerical studies [1–4] on perturbed flat bands indicate the existence of two different types of transitions: an inverse Anderson transition [1], independent of disorder strength, in weak disorder regime (below a system-specific disorder strength, say w_0) and a standard Anderson transition in strong disorder regime [5,6]. The different nature of these transitions originates from two types of scattering mechanisms prevailing in the regimes. The wave-function interference for $w < w_0$ is caused by strong backscattering due to diverging effective mass (vanishing group velocity of the wave function) and is insensitive to disorder strength (disorder-dependent scattering being weaker) [1,2]. The interference effects for $w > w_0$ are, however, due to disorder-dominated scattering, resulting in a transition at a specific disorder if the band is single particle [5]. In case of many-particle bands, the system in the $w > w_0$ regime undergoes a many-body localization transition at one or more critical disorder strengths [7–9]. A theoretical formulation of the transition in weak disorder regime and its connection with the one in strong disorder regime has been missing so far. Our objective here is to pursue a statistical route, analyze these transitions using spectral statistics as a tool, and present an exact mathematical formulation of the transition parameter in terms of the system conditions. The latter helps in identifying the universality class of the spectral statistics at each type of transition and reveals analogies if any exist.

The need to analyze the transition through statistical approach can be explained as follows. The standard search of a localization to delocalization transition, hereafter referred as LD transition, in a disordered system is based on a range of criteria, e.g., the existence of an order parameter, a divergence of correlation length at the critical point, a scaling behavior for finite system sizes, and critical exponents of the average physical properties. For complex systems, however, the fluctuation of physical properties, from one sample to another or even within one sample subjected to a perturbation, is often comparable to their average behavior and their influence on the physical properties can not be ignored. As a consequence, one has to consider criteria based on the distribution of the physical properties [5]. In case of systems where the physical properties can in principle be expressed in terms of the eigenvalues and eigenfunctions of a relevant linear operator, it is appropriate to seek criteria based on their joint probability distribution function (JPDF) [5].

The definition of criticality in a JPDF of N variable $x_1, \ldots, x_N$ is in general based on a single-parameter scaling concept [5]. The distribution $P(x_1, \ldots, x_N; t_1, \ldots, t_n)$ that depends on system size N and a set of n parameters $t_1, t_2, \ldots, t_n$ obeys one-parameter scaling if for large N it is approximately a function of only variables $x_1, \ldots, x_N$ and one scale-dependent parameter, say, $\Lambda \equiv \Lambda(N, t_1, \ldots, t_n)$. For system conditions under which the limit $\Lambda^* = \lim_{N\to\infty} \Lambda(N)$ exists, the distribution approaches a universal limiting form $P^*(\{x\}, \Lambda^*) = \lim_{N\to\infty} P(\{x\}, \Lambda)$ and is referred as critical with Λ^* as the critical parameter [5]. In [10], we considered a typical disorder perturbed flat band, with its Hamiltonian modeled by a system-dependent ensemble of Hermitian random matrices and described a single-parametric formulation of its ensemble density. As an integration of the ensemble density over all eigenfunction leads to the JPDF of its eigenvalues, this encourages us to search for a single-parametric scaling of the JPDF as well

as higher-order eigenvalue correlations. The universal limit of these correlations, if it exists, is referred as the critical spectral statistics for the ensemble.

The concept of critical spectral statistics was first introduced in [11] in context of metal-insulator transition in disordered Hamiltonians; the study showed that the distribution $P(s)$ of the spacings s between the nearest-neighbor eigenvalues of the Hamiltonian turns out to be a universal hybrid of the Wigner-Dyson distribution at small s and Poisson at large s, with an exponentially decaying tail: $P(s) \sim e^{-\kappa s}$ for $s \gg 1$ with κ as a constant [11]. The analytical studies later on indicated the criticality to manifest also through an asymptotically linear behavior of the number variance $\Sigma^2(r)$ (the variance in the number of levels in an spectrum interval of length rD) in mean number of levels r with a fractional coefficient [12].

As indicated by many studies of the transition in disordered systems, with or without particle interactions, the wave functions at the critical point are multifractal [5,6,13]. (Note, however, the study [14] claims an absence of multifractal wave functions in many-body systems; see [15] in this context.) This led to introduction of the singularity spectrum as the criteria for the criticality. The wave functions in the delocalized limit are essentially structureless and overlapping almost everywhere which leads to Wigner-Dyson–type level repulsion. In localized limit, the wave functions are typically localized at different basis state with almost negligible overlap which manifests in uncorrelated level statistics described by Poisson universality class. But, the multifractality leads to an intimate conspiracy between the correlations of energy levels and eigenfunctions (for both single-particle as well as many-particle type). This is because the two fractal wave functions, irrespective of their sparsity, still overlap strongly which in turn affects the decay of level correlations at long energy ranges. For $|e_n - e_m| \gg \Delta$, the correlation between two wave functions $\psi_n(r)$ and $\psi_m(r)$ at energies e_n and e_m is given as [12] $\langle |\psi_n(r)|^2 |\psi_m(r)|^2 \rangle \propto |e_n - e_m|^{1-(D_2/d)}$. In [12], χ was suggested to be related to the multifractality of eigenfunctions too: $\chi = \frac{d-D_2}{2d}$ with D_2 as the fractal dimension and d as the system dimension. However, numerical studies later on indicated the result to be valid only in the weak-multifractality limit [6].

Our objective in this work is to analyze the criticality of the spectral statistics and eigenfunctions when a flat band is perturbed by the disorder. In [10], we analyzed the disordered tight-binding Hamiltonians, with at least one flat band in the clean limit, using their matrix representation in an arbitrary basis. Presence of disorder makes it necessary to consider an ensemble of such Hamiltonians; assuming the Gaussian disorder in onsite energies (and/or interaction strengths, hopping, etc.) and by representing the nonrandom matrix elements by a limiting Gaussian, the ensemble density, say $\rho(H)$ with H as the Hamiltonian, was described in [10] by a multiparametric Gaussian distribution, with uncorrelated or correlated matrix elements. Using the complexity parameter formulation discussed in detail in [16–20], the statistics of $\rho(H)$ can then be mapped to that of a single-parametric Brownian ensemble (BE) appearing between Poisson and Wigner-Dyson ensemble [20–25] (also equivalent to Rosenzweig-Porter model [26]). The mapping is achieved by identifying a rescaled complexity parameter of the BE with that of the disordered band. The mapping not only implies connections of the flat-band statistics with the BE but also with other complex systems under similar global constraints, e.g., symmetry conditions and conservation laws [27,28]. Additionally, as discussed in detail in [10], it also leads to a single-parametric formulation of the level density and inverse participation ratio of the perturbed flat band.

In case of the BEs, the existence of a critical statistics and multifractal eigenstates is already known [9,20]. Their connection with disorder perturbed flat bands suggests presence of criticality in the latter too. This is indeed confirmed by our results presented here which indicate existence of a critical statistics for all weak disorders and is therefore in contrast to a single critical point in the disorder driven Anderson transition. Although the disorder independence of the statistics of a weakly disordered flat band was numerically observed in previous studies [2,3,29], its critical aspects were not explored. Another feature different from the Anderson transition is the following: with increasing disorder, the spectral statistics in a flat band undergoes a Poisson → Brownian ensemble → Poisson transition, implying a localization → extended → localization transition of the eigenstates. As is well known, the standard Anderson transition undergoes a delocalization → localization transition with increasing disorder [19]. Notwithstanding these differences, the complexity parameter formulation predicts an Anderson analog of a weakly disordered flat band and also reveals its connection of to a wide range of other ensembles [27,28,30] of the same global constraint class; the prediction is verified by a numerical analysis discussed later in the paper. Although the theoretical analysis presented here is based on the Gaussian disorder in flat bands, but it can also be extended to other types of disorder [18].

The paper is organized as follows. The complexity parameter formulation for the ensemble density of a disordered tight-binding lattice, with at least one flat band in clean limit, is discussed in detail in [10]. To avoid the repetition, we directly proceed, in Sec. II, to review the complexity parameter formulation for the statistics of the eigenvalues and eigenfunctions. This formulation is used in Secs. III and IV to derive an exact mathematical expression for the transition parameter and seek criticality in the disorder perturbed flat bands; here, we also analyze the influence of other neighboring bands on the statistics. A detailed numerical analysis of our theoretical claims is discussed in Sec. V. The next section presents a numerical comparison of the spectral statistics of the disordered flat bands with two other disordered ensembles with dispersive bands, namely, the standard Anderson ensemble with onsite Gaussian disorder and Rosenzweig-Porter ensemble and confirms an analogy of their statistics for those system parameters which result in the same value of their complexity parameters. This in turn validates our theoretical claim regarding the existence of one-parameter-dependent universality class of statistics among disordered bands, irrespective of the underlying scattering mechanism, and more generally among complex systems subjected to similar global constraints, e.g., symmetry, conservation laws, etc. We conclude in Sec. VII with a brief summary of our main results.

II. CRITICALITY OF SPECTRAL STATISTICS AND EIGENFUNCTIONS

Consider the Hamiltonian H of a disorder perturbed tight-binding lattice with at least one flat band in the clean limit: $H = V + U$ with V and U as single-particle and two-particle interactions. By choice of a physically motivated N-dimensional basis, H can be represented as an $N \times N$ matrix, with N as a system-specific parameter [31]. Here, we consider a basis, labeled by vectors $|k\rangle$, $k = 1 \to N$, in which (i) H is Hermitian, (ii) matrix elements H_{kl} are either independent or only pair-wise correlated. (For example, for $U = 0$, a basis consisting of single-particle states, e.g., site basis can serve the purpose. Similarly, for $U \neq 0$ a many-body wave-function basis [8], e.g., many-body Foch basis of localized single-particle states or occupation-number basis, is appropriate [32]; see Sec. III of [10] for an example.)

Ensemble complexity parameter. As discussed in [10] along with a few examples, the statistical behavior of the H matrix, with entries H_{kl}, can be modeled by a multiparametric Gaussian ensemble if H_{kl} are either independent or pairwise correlated. Assuming $e_1, e_2, \ldots, e_N$ and $U_1, \ldots, U_N$ as the eigenvalues and eigenfunctions of H, the correlations among their various combinations can then be obtained, in principle, by an integration of the ensemble density, say $\rho(H)$, over those variables which do not appear in the combination. To study the effect of varying system conditions on the correlations, it is, however, easier as well as more informative to first derive an evolution equation of $\rho(H)$ which on integration leads to the evolution equations for the correlations. As described in [10], irrespective of the number of changing conditions, the diffusion of $\rho(H)$ undergoes a single-parametric evolution

$$\frac{\partial \rho}{\partial Y} = \sum_{k,l;q} \frac{\partial}{\partial H_{kl;q}} \left[\frac{g_{kl}}{2} \frac{\partial}{\partial H_{kl;q}} + \gamma \; H_{kl;q} \right] \rho, \tag{1}$$

where $g_{kl} = 1 + \delta_{kl}$ with δ_{kl} as a Kronecker delta function and γ is an arbitrary constant, marking the end of the diffusion. The diffusion parameter Y, referred as the ensemble complexity parameter, is a combination of all ensemble parameters of $\rho(H)$ and thereby contains the information about the system parameters.

A detailed derivation of Eq. (1) is technically complicated and is discussed in [17] for multiparametric Gaussian ensembles (also see [16,27]) and in [18] for multiparametric non-Gaussian ensembles. As an example, consider the case which can be modeled by the probability density $\rho(H, v, b) = C \exp[-\sum_{q=1}^{\beta} \sum_{k \leqslant l} \frac{1}{2v_{kl;q}} (H_{kl;q} - b_{kl;q})^2]$; here, q refers to the real ($q = 1$) or imaginary ($q = 2$) component of the variable, with β as their total number, and, the variances $v_{kl;q}$ and mean values $b_{kl;q}$ can take arbitrary values (e.g., $v_{kl;q} \to 0$ for nonrandom cases). Using Gaussian form of $\rho(H)$, it is easy to see that a specific combination $T\rho$ of the parametric derivatives, namely, $T\rho \equiv \sum_{k \leqslant l;q} [\frac{2}{(2-\delta_{kl})} \; x_{kl;q} \; \frac{\partial \rho}{\partial v_{kl;q}} - \gamma \; b_{kl;q} \; \frac{\partial \rho}{\partial b_{kl;q}}]$ can exactly be rewritten as the right side of Eq. (1) where $x_{kl;q} \equiv 1 - (2 - \delta_{kl})\gamma \; v_{kl;q}$. Clearly, the left side of Eq. (1) must satisfy the condition $T\rho = \frac{\partial \rho}{\partial Y}$ which on solving gives Y as follows [16,18]:

$$Y = -\frac{1}{\gamma \; N_\beta} \; \ln \left[\prod_{k \leqslant l} \prod_{q=1}^{\beta} |x_{kl;q}| \quad |b_{kl;q} + b_0|^2 \right] + \text{const} \tag{2}$$

with $N_\beta = \frac{\beta N}{2}(N + 2 - \beta) + N_b$ and N_b as the total number of $b_{kl;q}$ which are not zero. Further, $b_0 = 1$ or 0 if $b_{kl;q} = 0$ or $\neq 0$, respectively. Similarly, Y can be formulated for the case when the matrix elements of H are pairwise correlated; see [10] and Eq. (15) of [17].

Spectral density correlations: Spectral complexity parameter. The statistical measures of a spectrum basically correspond to the local fluctuations of spectral density around its average value and can in principle be obtained from the nth-order level-density correlations $R_n(e_1, e_2, \ldots, e_n; Y)$, defined as $R_n = \int \prod_{k=1}^{n} \delta(e_k - \lambda_k) \rho(H; Y) DH$. As mentioned in [10] (see Sec. II C therein), Eq. (1) is analogous to the Dyson's Brownian motion model of random matrix ensembles, also referred as Brownian ensemble [see Sec. 6.13 of [21] or Eq. (9.2.14) of [22]]. The latter describe the perturbation of a stationary Gaussian ensemble by another one with Y as a perturbation parameter (or mean-square off-diagonal matrix element of the perturbation). Following exactly the same steps, as used in the derivation of Eq. (6.14.21) in Sec. 6.14 of [21], a hierarchical diffusion equation for R_n can be derived by a direct integration of Eq. (1) over $N - n$ eigenvalues and entire eigenvector space (also see Sec. 8 of [23] or [20,24,25] for more information). The specific case of $R_1(e)$ was discussed in detail in [10]; it varies at a scale $Y \sim N\Delta_e^2$. The solution of the diffusion equation for $R_2(e_1, e_2)$ with Poisson initial conditions is discussed in [24] [see Eq. (48) therein]. Contrary to R_1, R_n with $n > 1$ undergo a rapid evolution at a scale $Y \sim \Delta_e^2$, with $\Delta_e(e)$ as the local mean level spacing in a small energy range around e. For comparison of the local spectral fluctuations around $R_1(e)$, therefore, a rescaling (also referred as *unfolding*) of the eigenvalues e_n by local mean level spacing $\Delta_e(e)$ is necessary. As discussed in detail in Sec. 6.14 of [21] in context of single-parametric Brownian ensembles, this leads to a rescaling of both R_n as well as the crossover parameter Y, with new correlations given as $\mathcal{R}_n(r_1, \ldots, r_n) = \lim_{N \to \infty} (\Delta_e)^n R_n(e_1, e_2, \ldots, e_n)$, where $r_n = e_n/\Delta_e$ and the rescaled crossover parameter Λ_e given as [see Eq. (6.14.12) of [21]]

$$\Lambda_e(Y, e) = \frac{|Y - Y_0|}{\Delta_e^2}. \tag{3}$$

As discussed in [16] (see Sec. I E therein) and [17] [see neighborhood of Eq. (53) therein], Eq. (3) also gives the rescaled parameter in context of multiparametric Gaussian ensembles. (This is expected because the latter include Gaussian Brownian ensembles as a special case.) As Y is a combination of all ensemble parameters, Λ_e can be interpreted as a measure of average complexity (or uncertainty) of the system measured in units of mean level spacing. This encourages us to refer Λ_e as the spectral complexity parameter. It must be noted that $\Lambda_e \to \infty$ leads to a steady state, i.e., Gaussian orthogonal ensemble (GOE) if H is real symmetric ($\beta = 1$) or Gaussian unitary ensemble (GUE) if H is complex Hermitian ($\beta = 2$),

$\Lambda_e \to 0$ corresponds to an initial state [16,17,20]. Also note that Δ_e here refers to the single-particle mean level spacing for the single-particle bands and many-particle level spacing in case of the many-particle bands.

In principle, all spectral fluctuation measures can be expressed in terms of $\mathcal{R}_n$; the spectral statistics as well as its criticality, therefore, depend on the system parameters and energy only through Λ_e. For system conditions under which the limit $\Lambda^* = \lim_{N\to\infty} \Lambda_e(N)$ exists, $\mathcal{R}_n$ approaches a universal limiting form $\mathcal{R}_n{}^*(r_1, \ldots, r_n; \Lambda^*) = \lim_{N\to\infty} \mathcal{R}_n(r_1, \ldots, r_n; \Lambda_e)$. Clearly, the size dependence of Λ_e plays an important role in locating the critical point which can be explained as follows. The standard definition of a phase transition refers to infinite system sizes (i.e., limit $N \to \infty$); the parameter governing the transition is therefore expected to be N independent in this limit. In general, both $Y - Y_0$ as well as Δ_e and therefore Λ_e can be N dependent. In finite systems, a variation of N therefore leads to a smooth crossover of spectral statistics between an initial state ($\Lambda_e \to 0$) and the equilibrium ($\Lambda_e \to \infty$); the intermediate statistics belongs to an infinite family of ensembles, parametrized by Λ_e. However, for system conditions leading to an N-independent value of Λ_e, say Λ^*, the spectral statistics becomes universal for all sizes; the corresponding system conditions can then be referred as the critical conditions with Λ^* as the critical value of Λ_e. It should be stressed that the critical criteria may not always be fulfilled by a given set of system conditions; the critical statistics therefore need not be a generic feature of all systems. (For example, it is conceivable that Λ_e for a single-particle flat band perturbed by disorder may not achieve size independence at a specific energy for any disorder strength, thus indicating lack of criticality. Switching on particle interactions, however, may change the size dependence of Δ_e and Y and lead to a size independent Λ_e.) This indicates an important application of the complexity parameter based formulation: Λ_e provides an exact criteria, based only on a Gaussian ensemble modeling of the Hamiltonian, to seek criticality and predict the presence or absence of the LD transition in a disorder perturbed flat band (single particle as well as many particles).

At the critical value $\Lambda_e = \Lambda^*$, $\mathcal{R}_n$ (for $n > 1$) and therefore all spectral fluctuation measures are different from the two end points of the transition, i.e., $\Lambda_e = 0$ and ∞ and any one of them can, in principle, be used as a criterion for the critical statistics [20]. An important aspect of these measures is their energy dependence: $\mathcal{R}_n$ retain the dependence through Λ_e even after unfolding and are nonstationary, i.e., vary along the spectrum [20]. Any criteria for the criticality in the spectral statistics can then be defined only locally, i.e., within the energy range, say δe_c, in which Λ_e is almost constant [20]. For example, as reported by the numerical study [2] of diamond lattice with two flat bands, the metal-insulator transition occurs only at specific energies; this energy dependence of transition can theoretically be explained using Λ_e (see Sec. IV for details).

Spectral fluctuations: Standard measures. Based on previous studies, numerical as well as theoretical, two spectral measures, namely, nearest-neighbor spacing distribution $P(s)$ and the number variance $\Sigma^2(r)$, are confirmed to be reliable criteria for seeking criticality [5,6,11,22,33] in a wide range of complex systems. Here, $P(s)$ measures the probability of a spacing s between two nearest-neighbor energy levels (rescaled by local mean level spacing) and $\Sigma^2(r)$ gives the variance of the number of levels in an interval of r unit mean spacings. Although in the past $P(s)$ has played an important role in spectral fluctuation analysis of many-body systems, e.g., nuclei, atoms, and molecules, the numerical rescaling of a many-body spectrum is subjected to technical issues, e.g., exponentially increasing density of states or numerical simulation of large number of realization. This has motivated some recent studies to suggest another spectral measure for the short-range correlations, namely, distribution of the level spacing ratio [32,34]. In this study, however, it is sufficient to consider $P(s)$ for the critical analysis (this is because the disordered systems used in our, as well as previous, numerical analysis [2] are single-particle cases with Gaussian mean level densities and the unfolding on the spectrum is easier).

As confirmed by several studies in past (see, for example, [5,6,22,33] and references therein), the level fluctuations of a system in a fully delocalized wave limit behave similar to that of a Wigner-Dyson ensemble, i.e., GOE ($\beta = 1$) for cases with time-reversal symmetry and integer angular momentum and GUE ($\beta = 2$) for cases without time-reversal symmetry; here, $P(s) = A_\beta s^\beta e^{-B_\beta s^2}$ with $A_1 = \pi/2$, $B_1 = \pi/4$, $A_2 = 32/\pi^2$, $B_2 = 4/\pi$, and $\Sigma^2(r) = \frac{2}{\pi^2\beta}\left(\ln(2\pi r) + \gamma + 1 + \frac{(\beta-2)\pi^2}{8}\right)$ with $\gamma = 0.5772$. Similarly, the fully localized case shows a behavior typical of a set of uncorrelated random levels, that is, exponential decay for $P(s)$, also referred as Poisson distribution $P(s) = e^{-s}$, and $\Sigma^2(r) = r$ [5,22,33]. (In case of the structured matrices, e.g., those with additional constraints aside from Hermiticity, however, Poisson spectral statistics may appear along with delocalized eigenfunctions [35].)

For nonzero, finite Λ_e cases, the exact $P(s)$ behavior is known only for the Brownian ensembles consisting of matrices of size $N = 2$. As derived in [36], $P(s)$ for Poisson $\to$ GOE crossover and Poisson $\to$ GUE crossover can be given as

$$P(s, \Lambda_e) = \frac{s}{4\Lambda_e} \exp\left(-\frac{s^2}{8\Lambda_e}\right) \int_0^\infty dx\, e^{-\frac{x^2}{8\Lambda_e} - x} I_0\left(\frac{xs}{4\Lambda_e}\right), \quad \beta = 1 \tag{4}$$

$$P(s, \Lambda_e) = \frac{s}{\sqrt{2\pi\Lambda_e}} \exp\left(-\frac{s^2}{8\Lambda_e}\right) \times \int_0^\infty dx\, \frac{1}{x}\, e^{-\frac{x^2}{8\Lambda_e} - x} \sinh\left(\frac{xs}{4\Lambda_e}\right), \quad \beta = 2 \tag{5}$$

with I_0 as the modified Bessel function [see Eqs. (5) and (11) of [36]]. Here, $\beta = 1$ case corresponds to Brownian ensemble of real-symmetric matrices which appear as a perturbed (or nonequilibrium) state of a Poisson ensemble by a Gaussian orthogonal ensemble (also referred as the Poisson $\to$ GOE crossover) and are good models for systems with time-reversal symmetry. Similarly, the $\beta = 2$ case corresponds to Brownian ensembles of complex Hermitian matrices, appearing as a perturbed state of a Poisson ensemble by a Gaussian unitary

ensemble (also referred as Poisson → GUE crossover) and are applicable to systems without time-reversal symmetry. As $P(s)$ is dominated by the nearest-neighbor pairs of the eigenvalues, this result is a good approximation also for $N \times N$ case derived in [37], especially in small-s and small-Λ_e limits. Using the complexity parametric based mapping of the multiparametric Gaussian ensembles of the perturbed flat bands to Brownian ensembles, the above results can directly be used for the former case too.

As mentioned above, Λ_e is nonzero, finite, and size independent in the critical regime. This, along with Eqs. (4) and (5), indicates the following: $P(s) \sim e^{-\kappa s}$, for $s \gg 1$ with κ a constant for a finite Λ_e. The study [11] indicates an exponentially decaying tail of $P(s)$ as a criteria for critical spectral statistics. Similarly, $\Sigma^2(r)$ for the critical spectral statistics is linear but with fractional coefficient: $\Sigma^2(r) \sim \chi\, r$ with $0 < \chi < 1$ [5]. The coefficient χ, also referred as the level compressibility, is a characteristic of the long-range correlations of levels; it is defined as, in a range r around energy e, $\chi(e, r) = 1 - \int_{-r}^{r} [1 - R_2(e, e + s)]\, ds$. As $R_2(e, r)$ is related to $\Sigma_2(e, r)$, χ can also be expressed as the r rate of change of $\Sigma_2(e, r)$ [5,12]: $\chi = \lim_{r\to\infty} \frac{d\Sigma^2(r)}{dr}$. As discussed in [19,20], χ at the critical point Λ^* can be given as

$$\chi \approx 1 - 4\,\pi^2\,\Lambda^* \qquad \text{small } \Lambda^* \tag{6}$$

$$\approx \frac{1}{\beta\pi^2\Lambda^*} \qquad \text{large } \Lambda^* \tag{7}$$

with $\chi(e, r, \Lambda = 0) = 1$ and 0 for Poisson and Wigner-Dyson (GOE if $\beta = 1$ or GUE if $\beta = 2$) limits, respectively. χ is also believed to be related to the exponential decay rate of $P(s)$ for large s: $\chi = \frac{1}{2\kappa}$. Although χ is often used as a measure for criticality of the statistics [5] but, as discussed in [20], its numerical calculation in case of nonstationary ensembles is error prone and unreliable.

Eigenfunction fluctuation measures. At the critical point, the fluctuations of eigenvalues are in general correlated with those of the eigenfunctions. The spectral features at the criticality are therefore expected to manifest in the eigenfunction measures too. As shown by previous studies [5,6], this indeed occurs through large fluctuations of their amplitudes at all length scales, and can be characterized by an infinite set of critical exponents related to the scaling of the ensemble-averaged, generalized inverse participation ratio (IPR), i.e., moments of the wave-function intensity with system size. At transition, ensemble average of IPR, later defined as $\mathcal{I}_q(e) = \int |\Psi(\mathbf{r})|^{2q} d\mathbf{r}$ for a state $\Psi(\mathbf{r})$ with energy e, reveals an anomalous scaling with size N: $\langle \mathcal{I}_q \rangle(e) \sim N^{-(q-1)D_q/d}$ with D_q as the generalized fractal dimension of the wave-function structure and d as the system dimension. At critical point, D_q is a nontrivial function of q, with $0 < D_q < d$. The criticality in the eigenfunction statistics also manifests through other eigenfunction fluctuation measures, e.g., IPR distribution or two-point wave-function correlations [6]. A complexity parameter based formulation for these measures is discussed in [10,20,25].

Role of dimensionality. The dimensionality dependence of the critical point in the localization → delocalization transitions of the wave functions is well established. This can also be seen through Λ_e based formulation where dimension d of the system enters mainly through local mean level spacing $\Delta_e(e)$ at energy e. This can be explained as follows. In the delocalized regime, a typical state, say $\Psi(\mathbf{r})$, occupies the volume L^d with L as the linear size of the system which gives $|\Psi(\mathbf{r})|^2 = \frac{1}{L^d}$ [under normalization $\int_{L^d} |\psi(\mathbf{r})|^2\, d\mathbf{r} = 1$). As almost all states in this regime occupy the same space with unit probability, $\Delta_e(e) = \frac{1}{\langle \rho_e \rangle\, L^d}$ with $\langle \rho_e(e) \rangle$ as the mean spectral density (i.e., number of states per unit energy per unit volume): $\langle \rho_e(e) \rangle = \frac{1}{N} \langle \sum_{n=1}^{N} \delta(e - e_n) \rangle = \frac{R_1}{N}$. In the localized regime, the states are typically not overlapping but localized in the same regime with a probability $\frac{\xi^d}{L^d}$ where ξ is the average localization length at energy e; consequently, $\Delta_e(e)$ in this case corresponds to the level spacing in the localized volume ξ^d and is given as $\Delta_e(e) = \frac{1}{\langle \rho_e \rangle\, \xi^d} = \frac{N}{R_1\, \xi^d}$. Note $\xi(e)$ is in general a function of dimensionality [5] (aside from other system conditions, e.g., particle interactions) and can be expressed in terms of the inverse participation ratio $\overline{\langle \mathcal{I}_2 \rangle}$ of the eigenfunctions in a small neighborhood of e (with $\langle \ldots \rangle$ and $\overline{\cdots}$ implying ensemble and spectral averages, respectively): $\xi^d = (\overline{\langle \mathcal{I}_2 \rangle})^{-1}$. The above gives $\Delta_e(e) = \frac{N}{R_1}\, \overline{\langle \mathcal{I}_2 \rangle}$ which on substitution in Eq. (3) results in

$$\Lambda_e(Y, N, e) = \frac{|Y - Y_0|}{N^2} \left(\frac{R_1}{\overline{\langle \mathcal{I}_2 \rangle}} \right)^2. \tag{8}$$

As is clear from the above, a size independence of $\Lambda_e(e)$, i.e., existence of $\Lambda^*(e)$ requires a subtle cancellation of size dependence among the ensemble complexity parameter Y, ensemble-averaged level density R_1, and inverse participation ratio $\mathcal{I}_2$ (single particle or many particle based on the nature of the band). Note, in case of a many-particle band, ξ refers to many-particle localization length, defined as the typical scale at which many-particle wave function decays and I_2 its inverse participation ratio.

In the following sections, we use Eq. (8) to derive Λ_e for three cases of disorder perturbed flat bands; R_1 and I_2 for these cases are derived in [10].

III. TRANSITION IN AN ISOLATED FLAT BAND

In [10], we obtained the ensemble complexity parameter Y for a perturbed flat band. For cases in which disorder w is the only parameter subjected to variation, Y turns out to be

$$Y - Y_0 = -\frac{1}{N} \ln |1 - w^2|, \tag{9}$$

where Y_0 corresponds to the unperturbed flat band ($w = 0$) and N is the number of energy levels in the band. As discussed in [10], the level density R_1 for an isolated flat band for arbitrary w is [Eq. (39) of [10]]

$$R_1(e; w) = \frac{N}{\sqrt{2\pi\, w^2}}\, e^{-\frac{e^2}{2w^2}}. \tag{10}$$

Further, the averaged inverse participation ratio $\overline{\langle \mathcal{I}_2 \rangle}(e)$ for arbitrary w and large N can be approximated as (see Sec. V B of [10])

$$\overline{\langle \mathcal{I}_2 \rangle} \approx \frac{6\pi\, u_0}{N\, E_c}\, e^{\frac{2\Lambda_I}{N}}\, e^{-\frac{4e}{E_c} + \frac{e^2}{2w^2}} \tag{11}$$

with u_0 as the local intensity at $e = 0$ and $\Lambda_I = \frac{4 \ln|1-w^2|}{E_c^2}$. Here, E_c is an energy scale associated with the range of level repulsion around e and can in general depend on e as well as w. Equation (11) is obtained by assuming $E_c \sim N^{-\mu}$ with $\mu \geqslant 0$ which is consistent with the definition of E_c; as discussed in [10], $E_c \sim E_{th}$ with E_{th} as the Thouless energy: $E_{th} \sim o(N^{-1})$ and $o(N^0)$ for the localized and delocalized dynamics, respectively, but in partially localized regime $E_{th} \sim \Delta(e) N^{D_2/d}$, with $\Delta(e) = (R_1(e))^{-1}$ as the mean level spacing at energy e, D_2 as the fractal dimension, and d as the physical dimension. Assuming $\Delta(e) \sim N^{-\eta}$ with η as a system-dependent power, this gives

$$E_c \sim N^{-(\eta d - D_2)/d} \tag{12}$$

and $\mu = (\eta d - D_2)/d$. With $0 \leqslant D_2 \leqslant d$, the assumption $\mu > 0$ is valid at least in flat-band regime where $\eta = 1$ [the latter follows from Eq. (10)].

Substitution of Eqs. (10) and (11) along with Eq. (9) in Eq. (8) leads to

$$\Lambda_e(Y, N, e) = \frac{N E_c^2}{72\pi^3 u_0^2} \frac{|\ln|1-w^2||}{w^2} e^{-\frac{16 \ln|1-w^2|}{N E_c^2}} e^{\frac{8e}{E_c} - \frac{2e^2}{w^2}}. \tag{13}$$

As is clear from the above, Λ_e depends on the energy e, disorder w, as well as energy scale E_c. To seek the critical point, it is necessary to find specific e and w values which results in a Λ_e size independent as well as different from the two end points: $\lim_{N\to\infty} \Lambda_e \neq 0, \infty$. For further analysis of Eq. (13), we consider following energy and disorder regimes:

Case $e \sim 0$. For large N and $E_c \sim N^{-\mu}$ with $0 < \mu \leqslant \frac{1}{2}$, one can approximate $e^{-\frac{16 \ln|1-w^2|}{N E_c^2}} \sim 1$. This along with Eq. (13) then implies disorder independence of Λ_e for $e\sqrt{2} < w < 1$: $\Lambda_e(Y, N, e) = \frac{N E_c^2}{72\,\pi^3\,u_0^2}$. Further for cases with $\mu = \frac{1}{2}$, Λ_e is also size independent, implying a critical spectral statistics in the bulk of the flat-band spectrum (i.e., $e \sim 0$). As indicated by our numerical analysis, $\eta = 1$, $D_2 \approx 1.18$ which gives $E_c \sim N^{-0.41}$ for the two-dimensional checkerboard lattice ($d = 2$) in weak disorder limit. The criticality of the spectral statistics is also confirmed by the size independence of the fluctuation measures [see parts (c) and (e) of Figs. 2 and 3]. The details are discussed later in Sec. V. (Note, for weak disorder, the checkerboard lattice has a perturbed flat band in the neighborhood of a dispersive band but the former can still be treated as isolated.)

For large w and finite N, Λ_e decrease smoothly with increasing w and therefore the spectral statistics near $e \sim 0$ again approaches Poisson limit, implying a lack of level repulsion. Further, in the limit $N \to \infty$, $\Lambda_e \to 0$ for any finite $w > 1$ which indicates a transition from critical statistics to Poisson at $w \approx 1$. As is clear from the above, the statistics undergoes an inverse Anderson transition in the disorder perturbed flat band, with fully localized states at zero disorder becoming partially localized for a weak disorder ($w < 1$ in our case). However, the usual Anderson transition sets in presence of strong disorder ($w \simeq 1$). In infinite-size limit $N \to \infty$, the statistics therefore shows two types of disorder driven critical behavior near $e \sim 0$: (i) at $w \sim 0$, Poisson $\to$ near GOE (or near GUE in presence of magnetic field) transition of the level statistics, (ii) at $w \sim 1$, the level statistics transits from near GOE/GUE $\to$ Poisson.

Case $e > 0$. For $w^2 < 2e^2$, the term $e^{-\frac{2e^2}{w^2}} \to 0$ which gives $\Lambda_e \to 0$ and Poisson statistics. But, for a fixed $e > 0$, $e^{-\frac{2e^2}{w^2}} \to 1$ with increasing w and consequently Λ_e increases too if $w < 1$. For $w > 1$, however, the contribution from other terms results in a decrease of Λ_e with increasing w. For finite N the statistics at $e > 0$ therefore changes from Poisson $\to$ GOE $\to$ Poisson with increasing w. An important point worth emphasizing here is an energy dependence of the spectral statistics for infinite system sizes ($N \to \infty$) and for weak disorder: critical near $e \sim 0$ if $E_c(e \sim 0) \propto \frac{1}{\sqrt{N}}$ but Poisson for $e > 0$ if $N\,E_c^2 \leqslant 1$ for $e > 0$. This suggests the existence of a mobility edge separating partially localized states from the localized states.

At this stage, it is relevant to indicate the following. As the level density for a flat band in clean limit can be expressed as a δ function, irrespective of whether the band is single- or many-particle type, the formulation derived in [10] remains valid for both types of bands (although Y for two cases is different). Similarly, the response of the average inverse participation ratio to weak disorder discussed in [10] is based on a knowledge of initial condition only and not on the presence or absence of interactions in the band; it is thus applicable for both types of bands too. This is, however, not the case for the spectral fluctuations which are governed by Λ_e and therefore dependent on the local mean level spacing Δ_e. For many-particle spectrum, Δ_e in general depends on many-particle localization length which can be varied by tuning either disorder or interactions. Thus, the size independence of many body Δ_e can be achieved in many ways which could as a result lead to more than one critical point.

IV. TRANSITION IN A FLAT BAND WITH OTHER BANDS IN THE NEIGHBORHOOD

In presence of other bands, the energy as well as size dependence of Λ_e, defined in Eq. (8) can vary significantly based on the neighborhood. As calculation of Λ_e requires *a priori* knowledge of the level densities and IPR, here we consider two examples for which these measures are discussed in [10].

(i) *Two flat bands*: As discussed in Sec. VI A [10], $R_1(e)$ can now be expressed as a sum over two Gaussians (originating from δ-function densities of two flat bands)

$$R_1(e; w) = \frac{N}{2\sqrt{2\pi w^2}} \sum_{k=1}^{2} e^{-\frac{(e-e_k)^2}{2w^2}} \tag{14}$$

with e_1, e_2 as the centers of two flat bands. The IPR in the large-N limit is (see Sec. VI B of [10])

$$\overline{\langle \mathcal{I}_2 \rangle}(e, \Lambda_I) \approx \frac{3\,u_0\sqrt{2\pi}}{2\,R_1\,E_c} \sum_{k,l=1}^{2} e^{-\frac{4(e-e_k)}{E_c}} e^{-\frac{(e_l-e_k)^2}{2w^2} + \frac{2\Lambda_I}{N}} \times \Theta(e - e_k) \tag{15}$$

with $\Lambda_I = \frac{4 \ln|1-w^2|}{E_c^2}$ and $\Theta(x)$ as the step function: $\Theta(x) = 0, 1$ for $x < 0$ and $x > 0$, respectively. Substitution of Eqs. (14) and (15) in Eq. (8) now gives Λ_e for this case.

A better insight can, however, be gained by deriving Λ_e in different energy regimes.

Case $e \sim e_k$. For $e \sim e_k$, with $k = 1, 2$, Eqs. (14) and (15) can be approximated as $R_1(e; w) \approx \frac{N}{2\sqrt{2\pi w^2}}[1 + e^{-\frac{(e_2-e_1)^2}{2w^2}}]$ and $\overline{\langle \mathcal{I}_2 \rangle}(e) \approx \frac{6\pi u_0}{N E_c}\, e^{\frac{8|\ln|1-w^2|}{N E_c^2}}$. These on substitution in Eq. (8) give

$$\Lambda_e(Y, N, e) \approx \frac{N E_c^2}{288\pi^3 u_0^2} \frac{|\ln|1-w^2||}{w^2} \frac{e^{-\frac{16\ln|1-w^2|}{N E_c^2}}}{\left[1 + e^{-\frac{(e_2-e_1)^2}{2w^2}}\right]^2}. \tag{16}$$

Clearly, similar to the single-band case, here again Λ_e is independent of disorder for $w < 1$ and in large-N limit but it rapidly decreases with larger disorder (for $w > 1$). Here again the size independence of Λ_e requires $E_c \propto \frac{1}{\sqrt{N}}$. For $w < 1$, the spectral statistics at the centers of two Gaussian bands (flat bands in clean limit) can therefore be critical as well as disorder independent only if $\mu = \frac{1}{2}$.

Case $e \sim (e_1 + e_2)/2$. For the energies midway between two bands, R_1 is very small for $w < 1$ but, contrary to band center, it increases with increasing w for $w > |e_1 - e_2|$: $R_1(\frac{e_1+e_2}{2}) = \frac{N}{\sqrt{2\pi w^2}}\, e^{-\frac{(e_2-e_1)^2}{8w^2}}$ and Eq. (15) gives $\overline{\langle \mathcal{I}_2 \rangle}(e) \approx \frac{6\pi u_0}{N E_c}\, e^{\frac{8\ln|1-w^2|}{N E_c^2}}\, e^{\frac{-2(e_2-e_1)}{E_c}}\, e^{\frac{(e_1-e_2)^2}{8w^2}}\, [1 + e^{\frac{-(e_1-e_2)^2}{2w^2}}]$. With $Y - Y_0$ given by Eq. (9), we now have

$$\Lambda_e(Y, N, e) = \frac{N E_c^2}{72\pi^3 u_0^2} \frac{|\ln|1-w^2||}{w^2}\, e^{-\frac{16\ln|1-w^2|}{N E_c^2}} \times \frac{e^{\frac{4(e_2-e_1)}{E_c}}\, e^{\frac{-(e_1-e_2)^2}{2w^2}}}{\left(1 + e^{\frac{-(e_1-e_2)^2}{2w^2}}\right)^2}. \tag{17}$$

As is clear from the above, here also Λ_e become N independent, thus implying critical statistics if $E_c \propto N^{-1/2}$. Note, however, the term $e^{\frac{-(e_1-e_2)^2}{2w^2}}$ present in Eq. (17) can result in the statistics different from that of $e \sim e_k$.

A case of two flat bands was studied in [2] for the three-dimensional hexagonal diamond lattice. The study indicates $D_2 \approx 2.55$ and 2.61 for $e \sim e_k$ and $e \sim (e_1 + e_2)/2$, respectively. With $\Delta(e) \propto N^{-1}$ and $d = 3$, Eq. (12) gives E_c for this system as $N^{-0.15}$ for $e \sim e_k$ and $N^{-0.13}$ for $e \sim (e_1 + e_2)/2$. Based on our theory, the statistics is predicted to be size as well as disorder dependent near $e \sim (e_1 + e_2)/2$ and size dependent but disorder independent near $e \sim e_k$. The display in Figs. 4 and 5 of [2] indeed confirms this prediction.

The case of three flat bands was discussed in [38], for a bipartite periodic lattice described by a tight-binding, interacting Hamiltonian. The study indicates a localization → delocalization transition at the onset of disorder or many-body interactions. The possibility of a critical behavior for this case can be explored along the same route as given above.

(ii) *A flat band at the edge of a dispersive band*: For the combination of a flat band located at $e = 0$ and a dispersive band at $e > 0$ with the level density $f_d(e)$, the results in Sec. VI of [10] give

$$R_1(e; w) = \frac{N}{2\sqrt{2\pi w^2}}\, e^{-\frac{e^2}{2w^2}} + \frac{N}{2}\, f_w(e, w, N) \tag{18}$$

with $f_w(e, w, N)$ as the dispersive band density at disorder w and

$$\overline{\langle \mathcal{I}_2 \rangle}(e, \Lambda_I) \approx \frac{1}{2\,R_1} \frac{3\sqrt{2}}{w\,E_c} [u_0\sqrt{\pi} + B_1 + B_2 + B_3] \times e^{-\frac{4e}{E_c} + \frac{2\Lambda_I}{N}} \tag{19}$$

with $B_1 = \frac{2u_0 w}{E_c}\sqrt{\frac{\pi N}{\Lambda_I}} \int_{-\infty}^{\infty} dx\, f_w(x)\, e^{-\frac{2Nx^2}{\Lambda_I E_c^2} + \frac{4x}{E_c}}$, $B_2 = N \int_{-\infty}^{\infty} dx\, f_w(x) u_d(x)\, e^{-\frac{x^2}{2w^2} + \frac{4x}{E_c}}$, $B_3 = \sqrt{2\pi w^2} \int_{-\infty}^{\infty} dx\, f_w(x) u_d(x)\, e^{\frac{4x}{E_c}}$ and $\Lambda_I = \frac{4\ln|1-w^2|}{E_c^2}$. Here, u_0 and $u_d(e, w)$ are the local eigenfunction intensities in the flat band at disorder $w = 0$ and in dispersive band at disorder w. For cases in which $f_w(e, w, N)$ vary slower than the Gaussians in the related integrals, B_1 and B_2 can be approximated as follows: $B_1 = \pi\sqrt{2} u_0 f_w(\frac{\Lambda_I E_c}{4}) e^{\frac{2\Lambda_I N}{N}}$, $B_2 = \sqrt{2\pi w^2} u_d(\frac{4w^2}{E_c^2})\, e^{\frac{8w^2}{E_c^2}}$.

A substitution of Eqs. (18) and (19) along with Eq. (9) in Eq. (8) gives Λ_e for arbitrary energy and disorder but here again it is instructive to analyze the behavior near specific energies,

Case $e \sim 0$. Due to almost negligible contribution for weak disorder from the dispersive part near $e \sim 0$, one can approximate $R_1 \approx \frac{N}{2\sqrt{2\pi w^2}}$ and $\overline{\langle \mathcal{I}_2 \rangle} \approx \frac{6\pi u_0}{N E_c}$ which in turn gives $\Lambda_e = \frac{N E_c^2}{288\pi^3 u_0^2}$. The latter is therefore again size as well as disorder independent indicating criticality near $e \sim 0$ for all weak disorders if $E_c \propto N^{-1/2}$. As intuitively expected, the behavior of spectral statistics near $e \sim 0$ and $w < 1$ in this case is analogous to that of the single flat-band case.

As mentioned in [3,10], the two-dimensional checkerboard lattice consists of a flat band and a dispersive band in a clean limit. Our numerical analysis of the system for $w < 1$ indicated $\Delta(e) \propto N^{-1}$ and $D_2 \sim 1.18$ [see Figs. 2(a) and 2(b) and 3(a) and 3(b) of this work and Fig. 4 of [10]], leading to $E_c \sim N^{-0.41}$ which implies $\overline{\langle \mathcal{I}_2 \rangle} \sim N^{-0.59}$, an indicator of partially localized states [39]. Based on theoretical grounds, therefore, the spectral statistics is expected to be critical near $e \sim 0$ and $w < 1$; this is indeed confirmed by the size independence of the statistics displayed in Figs. 2(c) and 2(e) and 3(c) and 3(e).

For large w (e.g., $w > 1$ for the case with $\mu = \frac{1}{2}$), however, the contribution from the dispersive band becomes significant near $e \sim 0$. This results in $R_1(e \sim 0) \approx \frac{N}{2\sqrt{2\pi w^2}}\, T_1$ where $T_1 = 1 + \sqrt{2\pi w^2}\, f_w(0, w, N)$ and $\overline{\langle \mathcal{I}_2 \rangle} \approx \frac{6}{N}\frac{\sqrt{\pi}}{E_c\, T_1} [u_0\sqrt{\pi} + B_1 + B_2 + B_3]\, e^{\frac{8\ln|1-w^2|}{N E_c^2}}$. These on substitution in Eq. (8) give

$$\Lambda_e(Y, N, e) = \frac{N E_c^2}{288\,\pi^2} \frac{|\ln|1-w^2||}{w^2} \times \frac{T_1^4}{(u_0\sqrt{\pi} + B_1 + B_2 + B_3)^2} \times e^{-\frac{16\ln|1-w^2|}{N E_c^2}}. \tag{20}$$

As is clear from the above, for large w and finite N, Λ_e decrease smoothly with increasing w and therefore the spectral statistics near $e \sim 0$ again approaches the Poisson limit,

implying lack of level repulsion; note E_c is expected to decrease with increasing w. Further, in the limit $N \to \infty$, $\Lambda_e \to 0$ for any finite $w > 1$ which indicates a transition from critical statistics to Poisson at $w \approx 1$.

The above prediction is again consistent with our numerical analysis [see Figs. 4(c) and 4(e) and 5(c) and 5(e)]. Note as displayed in Fig. 5(a), $\Delta(e) \propto N^{-1}$, and in Fig. 5(b), $D_2 \approx 0.5$ which gives $E_c \sim N^{-0.75}$, thus implying a size dependent Λ_e, approaching zero in large-N limit which corresponds to Poisson statistics. Figures 4(c) and 4(e) and 5(c) and 5(e) indeed confirm the approach of spectral measures to Poisson limit for $e \sim 0$ and $w > 1$.

Case $e > 0$. Due to weaker contribution from the Gaussian density for $e > 0$, the contribution from the dispersive band density need not be negligible and it is appropriate to consider the full form of $R_1(e)$. The IPR can now be approximated as

$$\overline{\langle \mathcal{I}_2 \rangle} \approx \frac{6\sqrt{\pi}}{N E_c T_0} [u_0\sqrt{\pi} + B_1 + B_2 + B_3] e^{-\frac{4e}{E_c} + \frac{8 \ln|1-w^2|}{N E_c^2}}, \tag{21}$$

where $T_0 = e^{-\frac{e^2}{2w^2}} + \sqrt{2\pi w^2}\, f_w(e)$. The above leads to

$$\Lambda_e(Y, N, e) = \frac{N E_c^2}{288\pi^2} \frac{|\ln|1-w^2||}{w^2} \times \frac{T_0^4}{(u_0\sqrt{\pi} + B_1 + B_2 + B_3)^2} e^{-\frac{16 \ln|1-w^2|}{N E_c^2}} \times e^{\frac{8e}{E_c}}. \tag{22}$$

The presence of the term $e^{\frac{8e}{E_c}}$ in Eq. (22) results in the statistics different from the case $e \sim 0$. For $w = 0$, the

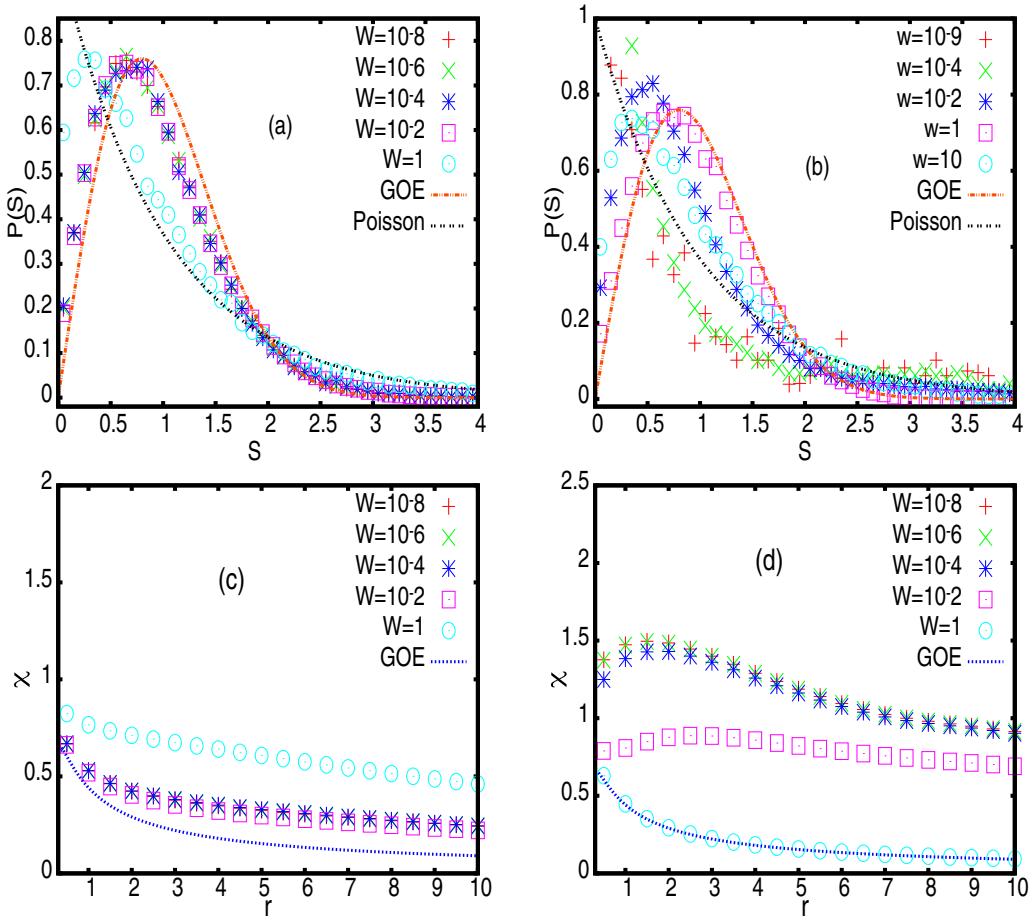

FIG. 1. Disorder dependence of spectral measures in two energy ranges: (a) $P(S)$ in the bulk of flat band ($e \sim 0$), (b) $P(S)$ in the bulk of dispersive band ($e \sim 4$), (c) $\chi(r)$ in the bulk of flat band ($e \sim 0$), (d) $\chi(r)$ in the bulk of dispersive band ($e \sim 4$). Here, $W = w^2$ and $P(S)$ refers to the distribution of the nearest-neighbor spacing S and $\chi(r)$ as the spectral compressibility for the unfolded eigenvalues taken from a narrow energy range around the specific energy for a fixed system size $L = 70$. The total number of eigenvalues used in each case is approximately 10^5. As clear from (a) and (c), the statistics is near GOE and disorder insensitive for $w < 1$ but approaches Poisson limit for $w > 1$. Clearly, with $w = 0$ as the Poisson case (due to degeneracy in flat-band spectrum), increasing disorder from zero leads to a change of statistics from Poisson to near-GOE to Poisson, which corresponds to a localization-delocalization-localization crossover of the eigenfunctions in the bulk of the flat band. But, (b) and (d) indicate a disorder insensitivity as well as inverse crossover in the dispersive band: with $w = 0$ as GOE case, increasing disorder from zero leads to a change of statistics from GOE → Poisson → GOE which corresponds to a delocalization-localization crossover of the eigenfunctions in the bulk of the dispersive band.

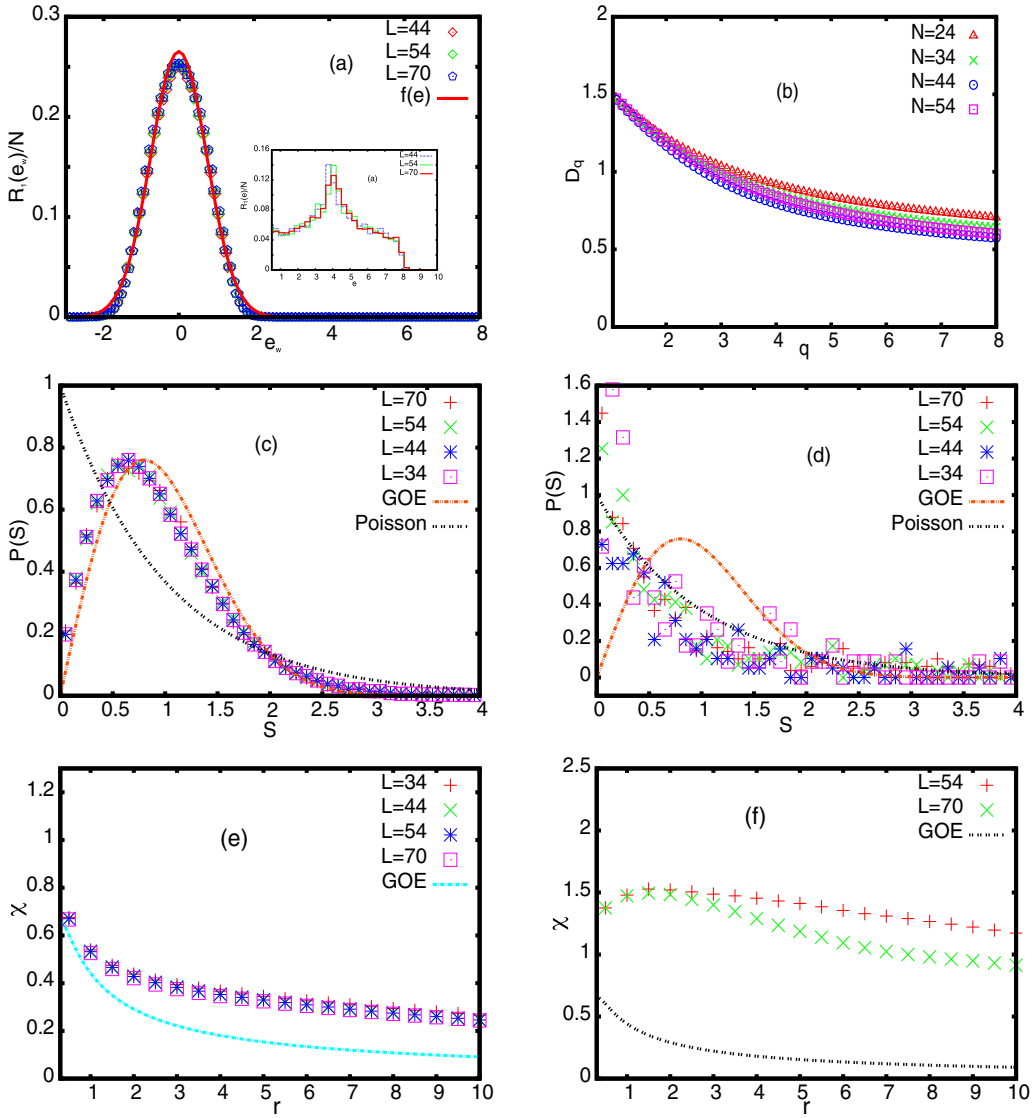

FIG. 2. Critical spectral statistics for weak disorder $w = \sqrt{3} \times 10^{-5}$: (a) Level density in the flat band (inset showing the behavior in the dispersive band) with fit $f(e_w) = \frac{1}{2\sqrt{1.25\pi}} e_w{}^{-0.8\, e_w^2}$, (b) D_q in the flat band ($e \sim 0$), (c) $P(S)$ for flat-band bulk ($e \sim 0$), (d) $P(S)$ for dispersive-band bulk ($e \sim 4$), (e) $\chi(r)$ for flat-band bulk ($e \sim 0$), (f) $\chi(r)$ for dispersive-band bulk ($e \sim 4$). Panels (c)–(e) also display the GOE and Poisson limits. Here, with $\langle \mathcal{I}_2 \rangle = 0.0116$ and $R_1 \approx \frac{0.248\, N}{w}$, Eq. (23) gives $\Lambda_e = 0.395$ near $e \sim 0$. The convergence of the curves for different sizes in (c) and (e) indicates scale invariance of the statistics in the flat band. The behavior is critical due to $P(S)$ being different from the two end points, namely, Poisson and GUE statistics even in large size limit. This is also confirmed by the χ behavior shown in (e), approaching a constant value 0.2 for large r, and D_q behavior shown in (b). Note the χ value is in agreement with Eq. (7) and D_2 is consistent with relation $D_2 = d(1 - 2\chi)$ with $d = 2$. The survival of scale invariance and partially localized behavior even for such a weak disorder indicates the critical point of the inverse Anderson transition to occur at zero disorder strength. In contrast, (d) and (f) indicate that the bulk statistics in the dispersive band is size dependent and is not critical.

statistics in the dispersive band at $e > 0$ is that of a GOE (or GUE if time-reversal symmetry is violated) but, with onset of disorder, it abruptly changes to Poisson. With increasing w for $0 < w < 1$, Λ_e increases but starts decreasing above $w = 1$. For large $e > 0$, the statistics therefore varies from GOE (at $w = 0$) to Poisson statistics for $w = 0^+$, becomes GOE at $w = 1$, and then again approaches Poisson $w > 1$. This prediction is consistent with our numerical results displayed in Figs. 2(d) and 2(f) and 3(d) and 3(f) for $w < 1$ and Figs. 4(d) and 4(f) and 5(d) and 5(f) for $w \gtrsim 1$.

V. NUMERICAL ANALYSIS: 2D CHECKERBOARD LATTICE

To verify our theoretical predictions, we pursue a numerical statistical analysis of the eigenvalues and eigenfunctions of the Hamiltonian $H = \sum_{x,y}^{N} V_{xy}\, c_y^\dagger . c_x$ of a 2D planar pyrochlore lattice with single orbital per site [3,10]. With 2D unit cell labeled as (m, n), one can write a site index as $x = (m, n, \alpha)$ with $\alpha = a, b$ (i.e., two atoms per unit cell). The lattice consists of one flat band $E_f = \varepsilon - 2t$ and

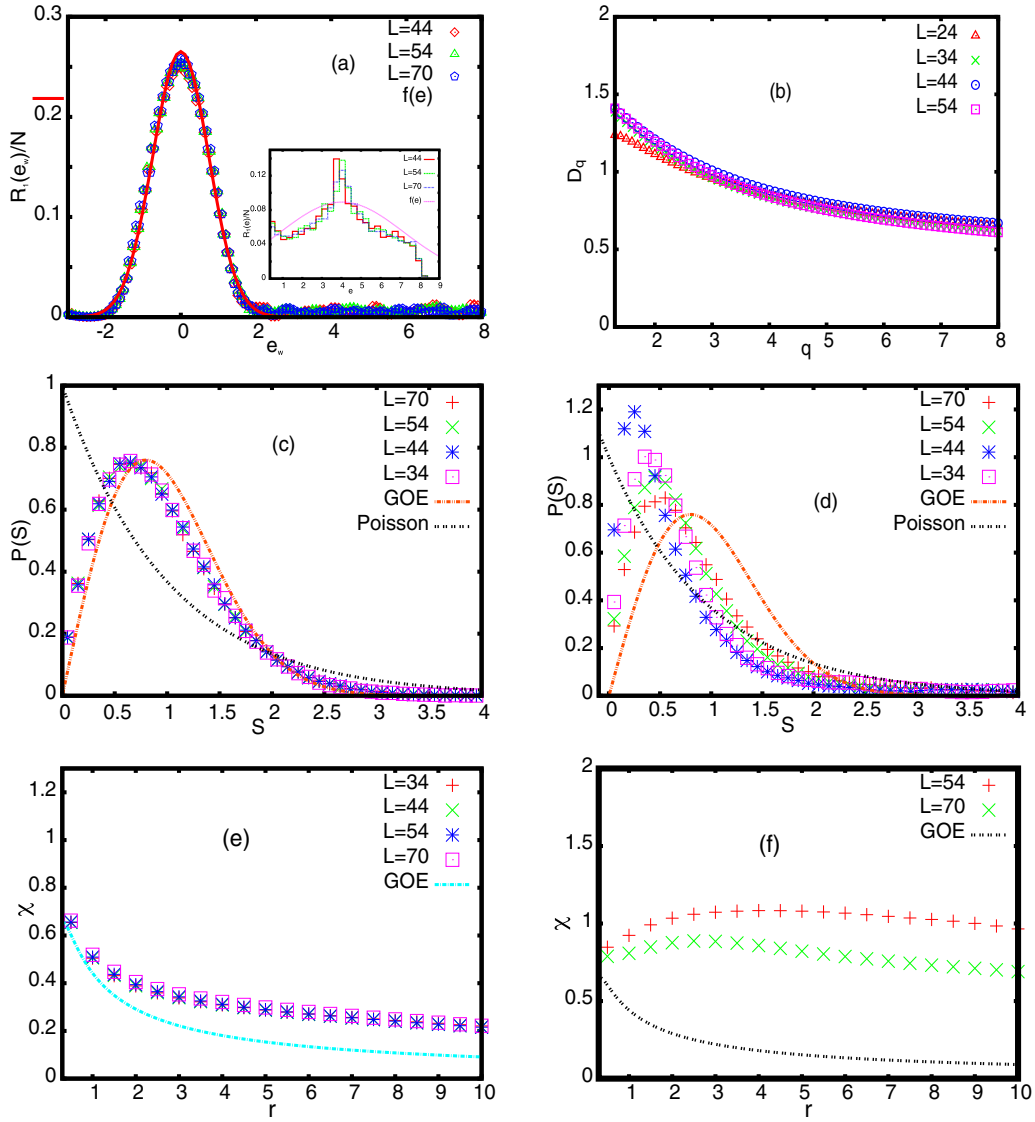

FIG. 3. Critical spectral statistics for weak disorder: $w = 0.1$: The details here are the same as in Fig. 2; the fit in part (a) is $f(e_w) = \frac{1}{2\sqrt{1.25\pi}} e^{-0.8e_w^2}$. Here, with $\langle \mathcal{I}_2 \rangle = 0.0116$ and $R_1(e) \approx \frac{0.248N}{w}$, Eq. (23) gives $\Lambda_e \approx 0.395$. As can be seen from (b) and (e), $\chi = 0.2$, $D_2 = 1.2$ near $e \sim 0$ which is again in agreement with Eq. (7) as well as relation $D_2 = d(1 - 2\chi)$ with $d = 2$. The analogy of the statistics with the case displayed in Fig. 2 indicates the disorder insensitivity of the statistics for $w < 1$.

one dispersive band $E_d = \varepsilon + 2t(\cos k_x + \cos k_y + 1)$ if V_{xy} satisfies the following set of conditions [3,10]: (i) $V_{xx} = \epsilon$, (ii) $V_{xy} = t$ with $x = (m, n, \alpha)$ if $y = (m, n, \beta)$ or $(m - 1, n, \beta)$ or $(m, n + 1, \beta)$ with $\beta = a, b$, and (iii) $V_{xy} = 0$ for all other x, y pairs.

For $\epsilon = 2$, $t = 1$, the Hamiltonian, in absence of disorder, consists of a flat band at $e = 0$ and a dispersive band centered at $e = 4$. (This can be seen from the band energies E_f and E_d given above.) The onset of disorder through onsite energies with $\langle V_{xx} \rangle = \varepsilon$, $\langle V_{xx}^2 \rangle - \langle V_{xx} \rangle^2 = w^2$ leads to randomization of the Hamiltonian. For the numerical analysis, therefore, we simulate large matrix ensembles of the Hamiltonian and, at many w, for various ensemble sizes M (the number of matrices in the ensemble) as well as the matrix sizes $N = L^2$. The energy sensitivity of the transition (due to energy dependence of Λ_e) requires the fluctuation's analysis at precisely a given value of energy. In order to improve the statistics, however, a consideration of the averages over an optimized energy range ΔE is necessary (not too large, to avoid mixing of different statistics). For comparison of a measure for different system sizes N at a given disorder, we have used only 20% levels in our numerical analysis.

In [10], we theoretically analyzed the disorder dependence of level density R_1 and average inverse participation ratio $\langle I_2 \rangle$. Our results indicated a disorder insensitivity of these measures in weak disorder limit ($w < 1$). This was also confirmed by their numerical analysis as well as that of D_q displayed in Fig. 4 of [10]. A search for criticality, however, also requires an analysis of the size dependence of the fluctuation measures. In this section, we numerically analyze the disorder and size dependence of the spectral fluctuations as well as the fractal dimensions D_q. Figure 1 displays the disorder dependence of $P(s)$ and $\Sigma^2(r)$ in two energy regimes, i.e., near $e \sim 0$ and $e \sim 4$ (corresponding to bulk of the flat band and dispersive

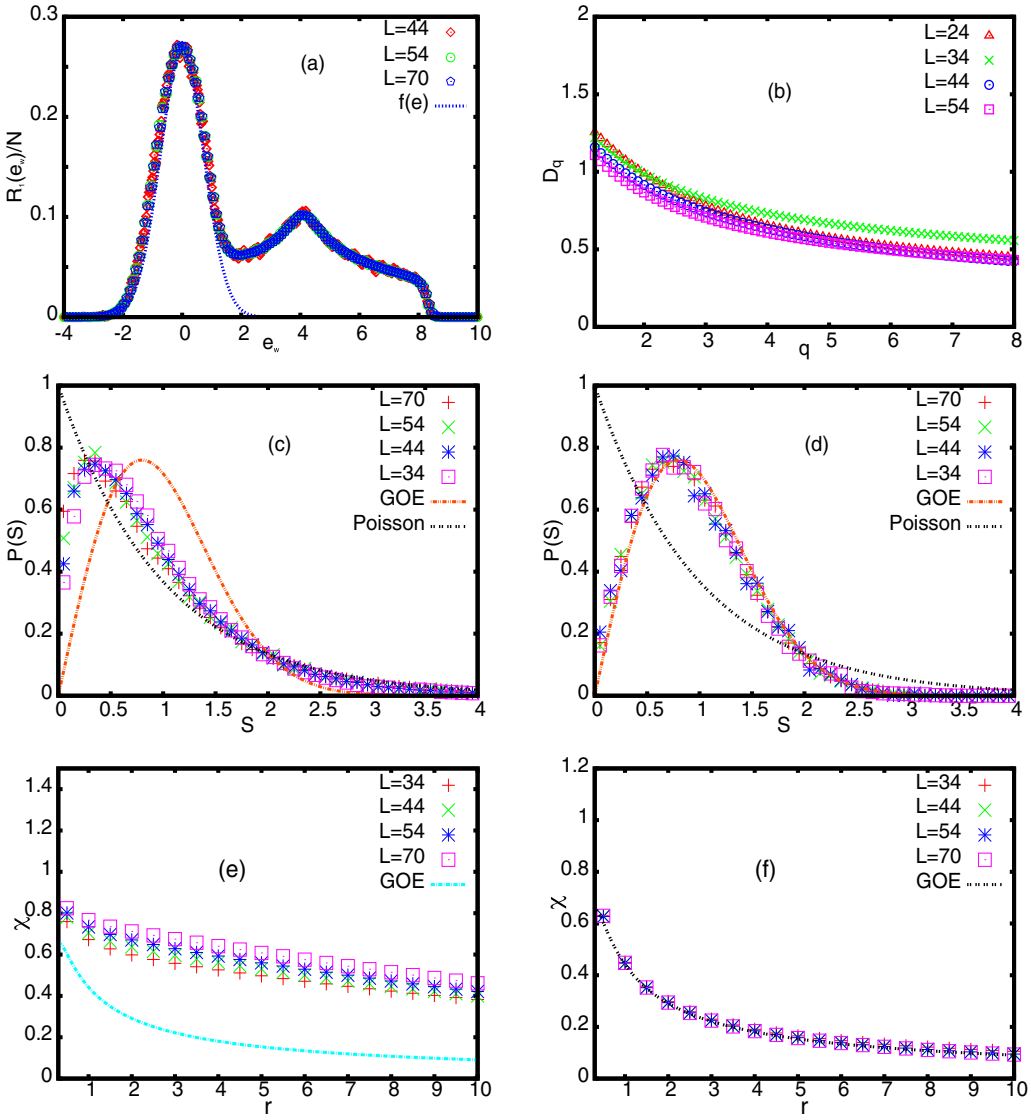

FIG. 4. Critical spectral statistics for disorder: $w = 1$: (a) Level density $R_1(e_w)/N$ along with fit $f(e_w) = \frac{1}{2\sqrt{1.15\pi}} e^{-0.76\, e_w^2}$ with $e_w = e/w$, (b) D_q near $e \sim 0$, (c) $P(S)$ near $e \sim 0$, (d) $P(S)$ near $e \sim 4$, (e) $\chi(r)$ near $e \sim 0$, (f) $\chi(r)$ near $e \sim 4$. Here, with $\langle \mathcal{I}_2 \rangle = 0.0269$ and $R_1(e) \approx \frac{0.261N}{w}$, Eq. (23) gives $\Lambda_e = 0.08$ near $e \sim 0$. Panels (b) and (e) now give $D_2 = 0.95$, $\chi = 0.5$ near $e \sim 0$; these values are no longer consistent with Eq. (6) or (7) or relation $D_2 = d(1 - 2\chi)$; the latter is, however, expected because the $D_2 - \chi$ relation is expected to be valid only for small χ. Further, as can be seen from (a), the two bands start merging at this disorder strength. In contrast to the weak disorder case, the statistics in flat and dispersive bands are now reversed, i.e., closer to Poisson and GOE, respectively. But, the survival of scale invariance and partially localized behavior even for this disorder strength indicates the dominance of flat-band spectrum on that of the dispersive band.

bands in clean limit). As clear from Figs. 1(a) and 1(c), for a weak disorder ($w < 1$) and near $e \sim 0$, both measures are insensitive to change in disorder. But as displayed in Figs. 1(b) and 1(d), the statistics in the dispersive band ($e \sim 4$) varies with disorder even for weak disorders. A similar result was reported by the numerical study of a three-dimensional disordered diamond lattice (with two flat bands in the clean limit) [2]. The effect of onsite disorder for the $\mathcal{T}_3$ lattice with three flat bands in clean limit was analyzed in [29]. The results again indicated disorder independence of the fluctuation measures for low disorder $w < 1$ but an increase of localization with w for $w > 1$.

Our next step is to seek criticality in the spectral and eigenfunction statistics. For this purpose, we focus on the size dependence of $P(S)$, χ, and D_2 in two energy regimes $e \sim 0$ and $e \sim 4$; the results for four disorder strengths, two in weak and two in strong disorder regime, are displayed in Figs. 2–5. [Here, for clarity of presentation, a comparison with theoretical approximation given by Eq. (4) is not displayed.] To determine Λ_e for these cases, it is numerically easier to use the following expression (instead of the theoretical approximation discussed in the previous section):

$$\Lambda_{e,\mathrm{FE}} = \frac{R_1^2}{\langle I_2 \rangle^2} \frac{|\ln|1 - w^2||}{N^3}, \tag{23}$$

where R_1 and $\langle I_2 \rangle$ are numerically obtained; the corresponding values are given in the captions of Figs. 2–5. Before proceeding further, it is important to note that the initial

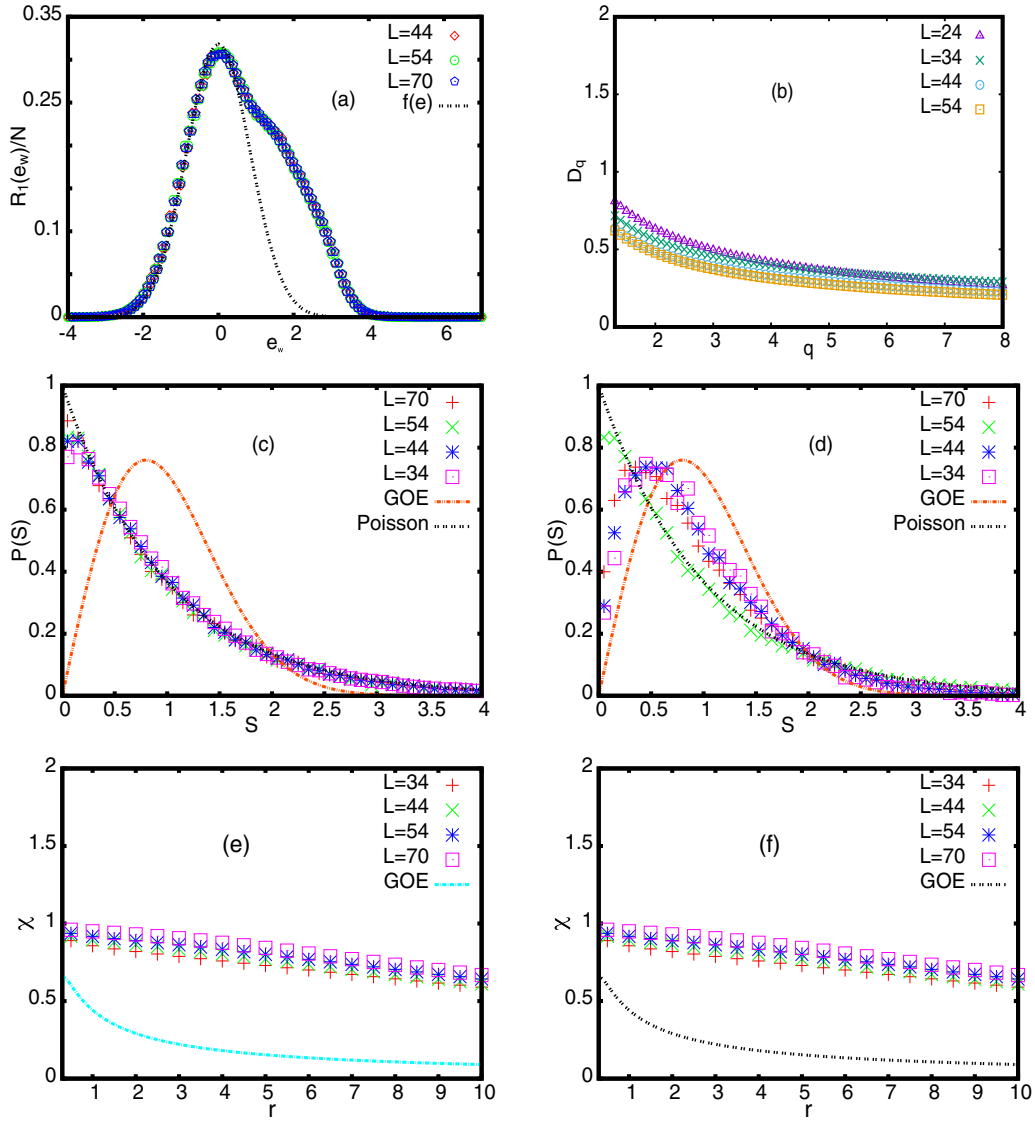

FIG. 5. Critical spectral statistics for strong disorder $w = \sqrt{10}$: (a) Level density $R_1(e_w)/N$ along with fit $f(e_w) = \frac{1}{2\sqrt{0.82\pi}} e^{-1.2\, e_w^2}$ with $e_w = e/w$, (b) D_q near $e \sim 0$, (c) $P(S)$ near $e \sim 0$, (d) $P(S)$ near $e \sim 4$, (e) $\chi(r)$ near $e \sim 0$, (f) $\chi(r)$ near $e \sim 4$. Here, with $\langle \mathcal{I}_2 \rangle = 0.1149$ and $R_1(e) \approx 0.3\ N/w$, Eq. (23) gives $\Lambda_e = 1.38 \times 10^{-3}$ near $e \sim 0$. As can be seen from (b) and (e), $\chi \approx 0.6$, $D_2 = 1.2$ near $e \sim 0$. Again, there is no agreement with Eq. (6) or relation $D_2 = d(1 - 2\chi)$. Clearly, Eq. (6) seems to be applicable for a much smaller Λ_e. Further, a large D_2 value here seems to be the effect of the complete merging between two bands giving rise to a new band. The statistics approaches the Poisson regime and an intermediate regime for $e \sim 0$ and $e \sim 4$, respectively, both indicating localized dynamics of wave functions. The system has now reached an insulator limit in the bulk energies but is still partially localized at the edge of the new band.

condition $w = 0$ (clean limit) corresponds to $\Lambda_e = 0$ but the initial state of the statistics is different in the two bands. In the clean limit, the flat band corresponds to Poisson statistics while the dispersive band corresponds to that of the GOE.

The size independence as well as location of the curves, intermediate to Poisson and GOE limits in Figs. 2(c) and 2(e), is an indicator of the critical spectral statistics; note the disorder here is very weak ($w \sim 10^{-5}$). Similarly, behavior in Fig. 2(b) is an indicator of the partially localized wave functions [6,39] in the weakly disordered flat-band bulk; also note that Figs. 2(b) and 2(e) give $D_2 \approx 1.2$ and $\chi \approx 0.2$, respectively, for the flat band which agrees well with the prediction based on the weak multifractality relation $D_2 = d(1 - 2\chi)$ (note $d = 2$ in our case) [12]. With $\Lambda_e \approx 0.384$ in this case (see caption of Fig. 2), the numerically obtained χ value is also consistent with Eq. (7). In contrast to behavior near $e \sim 0$, the size dependence of the measures is clearly visible from Figs. 2(d) and 2(f) (depicting behavior near $e \sim 4$) which rules out criticality in the dispersive regime. Furthermore, the statistics here is almost Poisson which indicates an abrupt transition from GOE (for $w = 0$) with onset of disorder;

As shown in Figs. 3(b), 3(c), and 3(e), the critical behavior in the flat band persists even when disorder is varied to $w \sim 10^{-1}$. But, in contrast to $w \sim 10^{-5}$, the statistics in the dispersive regime ($e \sim 4$) now shifts away from the Poisson limit [see Figs. 2(d) and 2(f) and 3(d) and 3(f)]; this implies a tendency of the wave functions in the dispersive band to in-

creasingly delocalize as w approaches 1. The results given in Figs. 2 and 3 clearly indicate the reverse trend of the statistics in two bands with increasing disorder in range $0 < w \leqslant 1$: the flat-band bulk undergoes a Poisson $\rightarrow$ near GOE $\rightarrow$ near Poisson type crossover with increasing w (though never reaching GOE), but the dispersive bulk changes from GOE $\rightarrow$ Poisson $\rightarrow$ GOE limit. For $w > 1$, however, bands increasingly overlap with each other and the statistics for both energy ranges approaches the Poisson limit with increasing disorder (although at different rate based on energy regime, see Figs. 4 and 5), as expected from a standard Anderson transition (later discussed in more detail in [6]). The statistics now seems to be size independent for all energy ranges. Also, note from Figs. 5(b) and 5(e), the relation $D_2 = d(1 - 2\chi)$ is no longer so well satisfied near $e \sim 0$ [here $d = 2$, $D_2 \approx 0.5$ from Fig. 5(b) and $\chi \approx 0.42$ from Fig. 5(e)]. This is expected because the multifractality in the band is no longer weak.

As confirmed by a large number of theoretical, numerical, as well as experimental studies of wide-ranging complex systems [5,6,22,33], Poisson and GOE type behaviors of the spectral statistics are indicators of localized and delocalized dynamics of the eigenfunctions, respectively, with an intermediate statistics indicating partially localized states [39] (note, as discussed in [35], the above relation between spectral statistics and eigenfunction dynamics is valid only for Hermitian matrices). This implies that, for $w \sim 10^{-5}$ and 10^{-1}, the states near $e \sim 0$ are extended (although not completely delocalized) but localized near $e \sim 4$ [see parts (c) and (d) of Figs. 2 and 3]. For $w = 1$, however, the localization tendency is now reversed, with almost localized states near $e \sim 0$ but delocalized near $e \sim 4$. This inverse eigenstate localization tendency at $e \sim 0$ to the at $e \sim 4$ for a given weak disorder hints at the existence of a mobility edge/region. Note beyond $w > 1$, all states are almost localized although the rate of change of localization length with disorder strength is energy dependent. (This follows because the average localization length in general depends on both disorder as well as energy.)

Let us now focus on the flat band only. As is clear from the above, the behavior near $e \sim 0$ indicates the occurrence of an inverse Anderson transition, with fully/compact localized states at zero disorder becoming partially localized for a nonzero weak disorder ($w < 1$ in our case). However, the usual Anderson transition sets in presence of the strong disorder (for $w \geqslant 1$). The quantum dynamics near $e \sim 0$ now shows two types of critical behavior: (i) at $w = 0$, a localized $\rightarrow$ extended state transition, in weak disorder regime, and (ii) an extended state $\rightarrow$ localization transition at $w \approx 1$.

VI. ANALOGY WITH OTHER ENSEMBLES

Based on the complexity parametric formulation, different ensembles subjected to the same global constraint (which is the Hermitian nature of H matrix in this study) are expected to undergo similar evolution. This in turn implies an analogy of their statistical measures if the values of their complexity parameters are equal and the initial conditions are statistically analogous. In this section, we verify the analogy by comparing the statistical behavior of weakly disordered flat bands with two other disordered ensembles of real-symmetric matrices, namely, the Anderson ensemble with onsite Gaussian disorder and Rosenzweig-Porter ensemble. Similar to flat-band lattices, both of these ensembles can be expressed as a multiparametric Gaussian ensemble and the expressions for Y and Λ_e for them can be easily obtained (see [19], [28], and [20] for details). The two ensembles can briefly be described as follows.

Anderson ensemble. The standard Anderson Hamiltonian $H = \sum_{k=1}^{N} \varepsilon_k c_k^\dagger c_k + \sum_{k,l=n.n}^{N} V_{kl} c_k^\dagger c_l$ describes the dynamics of an electron moving in a random potential in a d-dimensional tight-binding lattice with one atom per unit cell. The disorder in the lattice can appear through onsite energies ε_k or hopping V_{kl} between nearest-neighbor sites. Here, we consider the lattice with N sites, an onsite Gaussian disorder (with $\langle \varepsilon_k^2 \rangle = w^2$, $\langle \varepsilon_k \rangle = 0$), and a random nearest-neighbor hopping ($\langle V_{kl}^2 \rangle = t f_0$, $\langle V_{kl} \rangle = 0$ with $f_0 = 1$ if the sites k, l are nearest neighbors, otherwise it is zero) with z as the number of nearest neighbors. The ensemble density in this case can be written as

$$\rho(H) = \lim_{\sigma \to 0} C_a \prod_{k=1}^{N} e^{-\frac{H_{kk}^2}{2w^2}} \prod_{k,l=n.n}^{N} e^{-\frac{H_{kl}^2}{2t}} \prod_{k,l \neq n.n}^{N} e^{-\frac{H_{kl}^2}{2\sigma^2}} \tag{24}$$

with C_a as the normalization constant. From Eq. (9), the ensemble complexity parameter in this case is [19]

$$Y \approx -\frac{1}{N} \ln[|1 - w^2|\ |1 - 2t|^{z/2}] + \text{const.} \tag{25}$$

Here, the initial state is chosen as a clean lattice with sufficiently far off atoms resulting in zero hopping (i.e., both $w = 0$ and $t = 0$) which corresponds to a localized eigenfunction dynamics with Poisson spectral statistics. (This choice ensures the analogy of initial statistics with the flat-band case.) Substitution of Eq. (25) in Eq. (3) with $\Delta_e(e) = \frac{N\langle I_2 \rangle}{R_1}$ and $\overline{\langle I_2 \rangle}$ as the typical ensemble as well as spectral averaged IPR at e, leads to

$$\Lambda_{e,\text{AE}}(Y, N, e) = \frac{R_1^2}{N\ \overline{\langle I_2 \rangle}^2} \left|\ln(|1 - w^2|\ |1 - 2t|^{z/2})\right|. \tag{26}$$

Based on the complexity parameter formulation and verified by the numerical analysis discussed in [19], the level density here turns out to be a Gaussian: $R_1(e) = \frac{N}{\sqrt{2\pi\alpha^2}} e^{-\frac{e^2}{2\alpha^2}}$. As indicated by several studies in the past (e.g., [5,6]), the localization length ξ in this case depends on the dimensionality as well as disorder: (i) $\xi \approx \pi\ l \approx O(L^0)$ for all w for $d = 1$ with l as the mean-free path of the electron in the lattice, (ii) $\xi \approx e^{\frac{1}{2}\pi l k_F} \approx O(L^0)$ for all w for $d = 2$ with k_F as the Fermi wave vector, and (iii) $\xi \approx \xi_0(e, w)\ L^{D_2}$ with $D_2 = \frac{d}{2}$ for the critical disorder $w = w^*$ for $d > 2$. As a consequence, $\Lambda_e \sim O(1/N)$ for $d \leqslant 2$, which implies the statistics approaching an insulator limit $N \rightarrow \infty$. For $d > 2$, Λ_e in the spectral bulk is size independent only for $w = w*$ (for a fixed t), thus indicating only one critical point [19] of transition from delocalized to localized states with increasing disorder.

An important point worth reemphasizing here is that notwithstanding the N dependence of $Y - Y_0$ as for the Anderson ensemble (AE) and the flat bands (discussed in Sec. II), the statistics of energy levels and eigenfunctions in the two cases undergoes an inverse transition. This occurs because Λ_e,

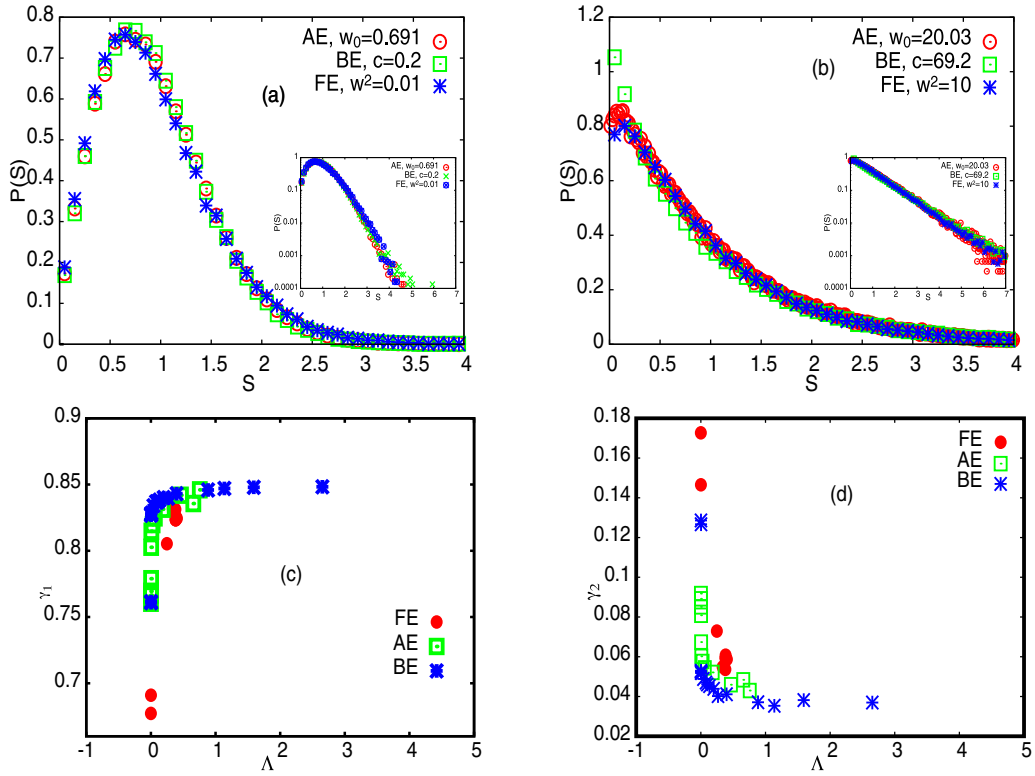

FIG. 6. Comparison of flat-band ensemble (FE) with AE and BE: Here, (a) and (b) display the $P(s)$ comparison for the AE, BE analogs of a weakly disordered flat band for two disorders $w^2 = 0.1$ and 10. The AE and BE analogs have been obtained by the conditions $\Lambda_{e,\mathrm{FE}} = \Lambda_{e,\mathrm{AE}} = \Lambda_{e,\mathrm{BE}}$ given by Eqs. (23), (26), and (28), respectively; the system parameter for the three ensembles leading to approximately same Λ_e near $e \sim 0$ are as follows: (a) FE: $N = 1156$, $w^2 = 10^{-2}$, $\varepsilon = 2$, $t = 1$, AE: $N = 512$, $w^2 = \frac{4.15}{6}$, $t = \frac{1}{12}$, BE: $N = 512$, $c = 0.2$, and (b) FE: $N = 1156$, $w^2 = 10$, $\varepsilon = 2$, $t = 1$, AE: $N = 512$, $w^2 = \frac{120.15}{6}$, $t = \frac{1}{12}$, BE: $N = 512$, $c = 69.2$. To rule out the accidental coincidence, we also compare $\gamma_1 = \gamma(0.4699)$, $\gamma_2 = \gamma(1.9699)$ for a range of Λ_e values. The results are displayed in (c) and (d), respectively. As clearly visible from the figures, the values for all three ensembles collapse on the same curve for small Λ_e values. But, while Λ_e of a flat band decreases for both small and large Λ_e, the Λ_e of an AE and BE smoothly increases from 0 to a large value with decreasing disorder. The deviation in their behavior for large Λ_e values is therefore an indicator of the different nature of transition.

the only parameter governing the spectral statistics, depends on the localization length and mean level density which have different response to disorder w in the two cases.

Rosenzweig-Porter (RP) ensemble. This represents an ensemble of Hermitian matrices with independent, Gaussian distributed matrix elements with zero mean, and different variance for the diagonals and the off diagonals. The ensemble density $\rho(H)$ in this case can be given as

$$\rho(H) \propto \exp\left[-\frac{1}{2}\sum_{i=1}^{N} H_{ii}^2 - (1+\mu_0)\sum_{i,j=1;i<j}^{N} H_{ij}^2\right]. \quad (27)$$

As is clear from the above, contrary to the multiparametric-dependent Anderson case, the RP ensemble depends on the single parameter, i.e., ratio of the diagonal to off-diagonal variance (aside from matrix size).

The ensemble density given above is analogous to the Brownian ensemble (BE) which arises due to a single-parametric perturbation of an ensemble of diagonal matrices by a GOE ensemble (discussed in detail in Sec. 2 of [19] and also in [20]). Clearly, the statistics of BE or RP ensemble lies between Poisson and GOE limits and depends on a single parameter which can be given as follows. The choice of initial condition as an ensemble of diagonal matrices (which corresponds to $\mu_0 \to \infty$) gives $Y - Y_0 = \frac{1}{4\mu_0}$ [see Eq. (11) of [19], also can be seen from Eq. (2) by substituting $v_{kl;q} = \delta_{kk} + \frac{(1-\delta_{kk})}{2(1+\mu_0)}\delta_{q1}$, $b_{kl,q} = 0$ for all k, l pairs) which leads to

$$\Lambda_{e,\mathrm{BE}}(e) = \frac{Y - Y_0}{\Delta_e(e)^2} = \frac{R_1^2}{4\mu_0}. \quad (28)$$

Note, the second equality in the above equation is obtained by using $\Delta_e(e) = \frac{1}{R_1(e)}$ (see [40] for a brief explanation).

As discussed in [20], the size dependence of $R_1(e;\mu_0)$ for a BE or RP ensemble changes from $\sqrt{N}$ to N. This in turn indicates the existence of two critical points: (i) for $\mu_0 = c_1 N^2$: here, $R_1 = \frac{N}{\sqrt{\pi}} e^{-e^2}$ which gives $\Lambda_{e,\mathrm{BE}} = \frac{1}{4\pi c_1} e^{-2e^2}$; (ii) for $\mu_0 = c_2 N$: here, $R_1(e) = (b\pi)^{-1}\sqrt{2bN - e^2}$ leading to $\Lambda(e) = \frac{2bN - e^2}{\pi^2 b^2 N c_2}$ with $b \sim 2$. The two critical points here correspond to a transition from localized $\to$ extended $\to$ delocalized states with decreasing μ_0 [20].

Parametric values for the analogs. For numerical analysis of the Anderson ensemble, we consider a three-dimensional cubic lattice with hard-wall boundary conditions, onsite Gaussian disorder w, and a random hopping with $t = \frac{1}{12}$. For the Brownian ensemble, we choose the case with $\mu_0 = cN^2$ (note the latter choice is arbitrary). The system parameters for

the Anderson and Brownian ensemble analogs of a weakly disordered flat band can now be obtained by invoking the following condition:

$$\Lambda_{e,\mathrm{FE}} = \Lambda_{e,\mathrm{AE}} = \Lambda_{e,\mathrm{BE}} \tag{29}$$

with $\Lambda_{e,\mathrm{FE}}$, $\Lambda_{e,\mathrm{AE}}$, $\Lambda_{e,\mathrm{BE}}$ given by Eqs. (23), (26), and (28), respectively.

Figure 6 displays a comparison of the nearest-neighbor spacing distribution for two cases of disordered checkerboard lattice (with Fermi energy in bulk of the flat band) with AE and BE analogs predicted by Eq. (29). The numerically obtained values for the analogs near ($e \sim 0$ for each case) are as follows:

(i) *Weak disorder analogy.* (a) FE: $N = 1156$, $w^2 = 0.01$, $\varepsilon = 2$, $t = 1$, $\langle I_2^{typ}\rangle = 0.0116$, $R_1(e) = \frac{0.248\ N}{w}$ which gives $\Lambda_{e,\mathrm{FE}} = 0.395$; (b) AE: $N = 512$, $w^2 = 4.15/6$, $t = 1/12$, $z = 6$, $\langle I_2^{typ}\rangle = 0.025$, $R_1 = 0.2983 \times N$ with $\Lambda_{e,\mathrm{AE}} = 0.465$; and (c) BE: $N = 512$, $c = 0.2$ with $\Lambda_{e,\mathrm{BE}} = 0.398$.

(ii) *Strong disorder analogy.* (a) FE: $N = 1156$, $w^2 = 10$, $\varepsilon = 2$, $t = 1$, $\langle I_2^{typ}\rangle = 0.1149$, $R_1(e) = \frac{0.3\ N}{w}$ which gives $\Lambda_{e,\mathrm{FE}} = 1.3 \times 10^{-3}$; (b) AE: $N = 512$, $w^2 = 120.15/6$, $\langle I_2^{typ}\rangle \approx 0.3$, $R_1 \approx 0.1/N$ with $\Lambda_{e,\mathrm{AE}} = 7.58 \times 10^{-4}$; and (c) BE: $N = 512$, $c = 69.2$ with $\Lambda_{e,\mathrm{BE}} = 1.15 \times 10^{-3}$.

The AE and BE analogs for the other flat-band cases can similarly be obtained. Alternatively, statistics of the perturbed flat band considered here can also be mapped to the AEs with different system conditions and the BE with $\mu_0 \propto N$. To confirm that this analogy is not a mere coincidence and exists for other Λ_e values too, we compare these ensembles for full crossover from $\Lambda_e = 0 \to \infty$. One traditionally used measure in this context is the relative behavior of the tail of nearest-neighbor spacing distribution $P(s)$, defined as

$$\gamma(\delta;\Lambda) = \frac{\int_0^\delta [P(s;\Lambda) - P(s;\infty)]ds}{\int_0^\delta [P(s;0) - P(s;\infty)]ds} \tag{30}$$

with δ as one of the two crossing points of $P_o(s) = P(s;\infty)$ and $P_p(s) = P(s;0)$ (here the subscripts o and p refer to the GOE and Poisson cases, respectively) [5,19]. As obvious, $\gamma = 0$ and 1 for GOE and Poisson limit, respectively, and a fractional value of γ indicates the probability of small spacings different from the two limits. In the limit $N \to \infty$, a γ value different from the two end points is an indicator of a new universality class of statistics and therefore a critical point. Figures 6(c) and 6(d) show a comparison of γ for two δ values for three systems: $\gamma_1 = \gamma(\delta_1)$ and $\gamma_2 = \gamma(\delta_2)$, with $\delta_1 = 0.4699$, $\delta_2 = 1.9699$; the display confirms our theoretical claim regarding the analogy of the three systems. It must be noted that the Λ_e for FE never approaches a value as large as that of AE and BE; following from Eqs. (13) and (17), it first increases and then decreases beyond a disorder-strength $w \sim 1$. This is contrary to AE and BE for which Λ_e decreases with increasing disorder. This behavior is also confirmed by our numerical analysis displayed in the figure.

VII. CONCLUSION

Finally, we summarize with main insights and results given by our analysis. We find that a disordered system, with one or more flat bands in the clean limit, can undergo two types of localization to delocalization transition. In the weak disorder regime (below a system-specific disorder strength, say w_c), the localization is insensitive to disorder strength and persists even for a very small disorder. This in turn leads to a critical spectral statistics, disorder independent and analogous to a Brownian ensemble intermediate to Poisson and Wigner-Dyson classes. But, in the strong disorder regime ($w > w_c$), the behavior is analogous to that of a disorder driven, standard Anderson transition (for single-particle bands) or many-body localization transition (for many-particle bands) in which a size-invariant spectral statistics occurs only at specific disorder strengths; the statistics here is again analogous to a Brownian ensemble but characterized by a different parameter value. This clearly reveals the influence the underlying scattering has on the transitions in the two regimes: although it affects the transition parameter dependence on disorder, the spectral statistics in both regimes belongs to one parameter-dependent universality class of Brownian ensembles.

The analysis presented here is based on a single-parameter formulation of the spectral statistics. This not only helps in theoretical understanding of the numerical results given by our, as well as previous, studies [2] but also reveals additional features. For example, it provides a unified formulation of the spectral statistics in the weak and strong disorder regimes (notwithstanding different scattering conditions). It also identifies the spectral complexity parameter as the transition parameter and leads to its exact mathematical expression, which in turn helps in the search of criticality in a disorder perturbed flat band; this occurs when the system conditions conspire collectively to render the spectral complexity parameter size independent. More clearly, the criticality requires the ensemble complexity parameter, an indicator of the average uncertainty in the system, measured in the units of local mean level spacing, to become scale free. The underlying localization dynamics clearly leaves its fingerprints on the transition parameter; the latter turns out to be disorder independent in the weak disorder regime but is disorder dependent in the strong disorder regime.

The advantage of complexity parameter based analysis goes beyond a search for criticality in perturbed flat bands. It also reveals an important analogy in the localization to delocalization crossover in finite systems: notwithstanding the difference in the number of critical points as well as equilibrium limits, the statistics of a disordered flat band can be mapped to that of a single-parametric Brownian ensemble [20] as well as a multiparametric Anderson ensemble [19] (see Sec. VI). The analogy of these ensembles to other multiparametric ensembles intermediate between Poisson and Wigner-Dyson is already known [18,20,27,30]. In fact, it seems a wide range of localization → delocalization transition can be modeled by a single-parameter Brownian ensemble appearing between Poisson and GOE (Rosenzweig-Porter ensemble) [28]. This hints at a large-scale universality and a hidden web of connection underlying complex systems even for a partially localized regime. Note the universality of spectral statistics and eigenfunctions in the ergodic or delocalized wave regime is already known but the complexity parameter formulation reveals a universality even at the critical point of widely different systems (of same global constraint class) if their complexity parameters are equal. It is relevant for the

following reason: It is well known that average properties of systems often show a power-law behavior at the critical point and can be classified into various universality classes based on their powers, referred as the critical exponents. However, in case of a complex system where the fluctuations of physical properties are often comparable to their averages, it is not enough to know the universality classes of critical exponents. An important question in this context is whether there are universality classes among the fluctuation properties too. As discussed in Sec. VI, such universality classes can indeed be identified based on the complexity parameter formulation. This issue will be discussed in more detail in a future publication.

Our study gives rise to many new queries. For example, an important question is whether weak particle-particle interactions in clean flat bands can mimic the role of weak disorder in the perturbed flat bands. At least, the complexity parameter formulation predicts this to be the case but a thorough investigation of the fluctuations is needed to confirm the prediction. A detailed analysis of the role of the symmetries in flat-band physics using the complexity parameter approach still remains to be investigated. Our analysis seems to suggest the existence of a mobility edge too, however, this requires a more thorough investigation. We expect to explore some of these questions in the future.

[1] M. Goda, S. Nishino, and H. Matsuda, Phys. Rev. Lett. **96**, 126401 (2006).

[2] S. Nishino, H. Matsuda, and M. Goda, J. Phys. Soc. Jpn. **76**, 024709 (2007).

[3] J. T. Chalker, T. S. Pickles, and P. Shukla, Phys. Rev. B **82**, 104209 (2010).

[4] D. Leykam, J. D. Bodyfelt, A. D. Desyatnikov, and S. Flach, Eur. Phys. J. B **90**, 1 (2017).

[5] M. Janssen, Phys. Rep. **295**, 1 (1998).

[6] A. D. Mirlin and F. Evers, Rev. Mod. Phys. **80**, 1355 (2008); F. Evers, A. Mildenberger, and A. D. Mirlin, Phys. Rev. B **64**, 241303 (2001).

[7] D. Basko, I. Aleiner, and B. Altshuler, Ann. Phys. (NY) **321**, 1126 (2006).

[8] C. Monthus and T. Garel, Phys. Rev. B **81**, 134202 (2010).

[9] V. E. Kravtsov, I. M. Khaymovich, E. Cuevas, and M. Amini, New. J. Phys. **17**, 122002 (2015).

[10] P. Shukla, Phys. Rev. B **98**, 054206 (2018).

[11] B. I. Shklovskii, B. Shapiro, B. R. Sears, P. Lambrianides, and H. B. Shore, Phys. Rev. B **47**, 11487 (1993).

[12] J. T. Chalker, V. E. Kravtsov, and I. V. Lerner, Pis'ma Zh. Eksp. Teor. Fiz. **64**, 355 (1996) [JETP Lett. **64**, 386 (1996)].

[13] M. Serbyn, Z. Papić, and D. A. Abanin, Phys. Rev. B **96**, 104201 (2017); M. Pino, V. E. Kravtsov, B. L. Altshuler, and L. B. Ioffe, *ibid.* **96**, 214205 (2017); X. Chen, X. Yu, G. Y. Cho, B. K. Clark, and E. Fradkin, *ibid.* **92**, 214204 (2015); D. J. Luitz, F. Alet, and N. Laflorencie, Phys. Rev. Lett. **112**, 057203 (2014); J. Lindinger and A. Rodríguez, Acta Phys. Pol. A **132**, 1683 (2017).

[14] Z. Gulacsi, Phys. Rev. B **69**, 054204 (2004); Z. Gulacsi, A. Kampf, and D. Vollhardt, Phys. Rev. Lett. **99**, 026404 (2007).

[15] The matrix representation of an operator depends on the choice of the basis and the constraints on the dynamics. This in turn also affects the behavior of the eigenfunctions (due to their basis dependence). Previous studies claiming multifractal eigenfunctions at a critical point are often concerned with Hamiltonian matrices with Hermiticity as the only constraint. For cases where the system is subjected to additional constraints, e.g., those resulting in positive-semidefinite matrices as in [14], further investigations are needed to confirm the mutifractality.

[16] P. Shukla, Phys. Rev. E **62**, 2098 (2000).

[17] P. Shukla, Phys. Rev. E **71**, 026226 (2005).

[18] P. Shukla, J. Phys. A: Math. Gen. **41**, 304023 (2008).

[19] P. Shukla, J. Phys.: Condens. Matter **17**, 1653 (2005).

[20] S. Sadhukhan and P. Shukla, Phys. Rev. E **96**, 012109 (2017).

[21] F. Haake, *Quantum Signatures of Chaos* (Springer, Berlin, 1991).

[22] M. L. Mehta, *Random Matrices*, 2nd ed. (Academic, New York, 1991).

[23] J. B. French, V. K. B. Kota, A. Pandey, and S. Tomsovic, Ann. Phys. (NY) **181**, 198 (1988).

[24] A. Pandey, Chaos, Solitons, Fractals **5**, 1275 (1995).

[25] P. Shukla, J. Phys. A: Math. Theor. **50**, 435003 (2017); Phys. Rev. E **75**, 051113 (2007).

[26] N. Rosenzweig and C. E. Porter, Phys. Rev. **120**, 1698 (1960).

[27] R. Dutta and P. Shukla, Phys. Rev. E **76**, 051124 (2007); **78**, 031115 (2008); M. V. Berry and P. Shukla, J. Phys. A: Math. Gen. **42**, 485102 (2009).

[28] P. Shukla, New J. Phys. **18**, 021004 (2016).

[29] J. Vidal, P. Butaud, B. Doucot, and R. Mosseri, Phys. Rev. B **64**, 155306 (2001); J. Vidal, G. Montambaux, and B. Doucot, *ibid.* **62**, R16294 (2000).

[30] P. Shukla and S. Sadhukhan, J. Phys. A: Math. Theor. **48**, 415002 (2015); S. Sadhukhan and P. Shukla, *ibid.* **48**, 415003 (2015).

[31] The formulation presented here is applicable for an arbitrary basis as long as the matrix remains Hermitian. However, the choice of a basis which preserves global constraints of the system, i.e., the symmetry and conservation laws can provide physically relevant information; for example, it permits a comparison of different complex systems (those with same global constraints) and reveals their statistical analogies through the complexity parameter formulation.

[32] V. Oganesyan and D. A. Huse, Phys. Rev. B **75**, 155111 (2007).

[33] T. Guhr, A. Muller-Groeling, and H. Weidenmuller, Phys. Rep. **299**, 189 (1998).

[34] Y. Y. Atas, E. Bogomolny, O. Giraud, and G. Roux, Phys. Rev. Lett. **110**, 084101 (2013); Y. Y. Atas, E. Bogomolny, O. Giraud, P. Vivo, and E. Vivo, J. Phys. A: Math. Theor. **46**, 355204 (2013).

[35] T. Mondal, S. Sadhukhan, and P. Shukla, Phys. Rev. E **95**, 062102 (2017); T. Mondal and P. Shukla, arXiv:1807.04173.

[36] V. K. B. Kota and S. Sumedha, Phys. Rev. E **60**, 3405 (1999); E. Caurier, B. Grammaticos, and A. Ramani, J. Phys. A: Math. Gen. **23**, 4903 (1990); G. Lenz and F. Haake, Phys. Rev. Lett. **67**, 1 (1991).

[37] S. Tomsovic, Bounds on the time-reversal non-invariant nucleon-nucleon interaction derived from transition-strength fluctuations, Ph.D thesis, University of Rochester, 1986; F. Leyvraz and T. H. Seligman, J. Phys. A: Math. Gen. **23**, 1555 (1990).

[38] J. Vidal, B. Doucot, R. Mosseri, and P. Butaud, Phys. Rev. Lett. **85**, 3906 (2000).

[39] The term partially localized state here refers to an eigenstate of the system which extends up to a few basis states only, say n, with $1 < n < N$ in an N-dimensional basis. It can then be characterized by an inverse participation ratio I_2 between zero and $1/N$. A fully localized state with this definition corresponds to the one confined to a single basis state and has $I_2 = 1$. Similarly, a delocalized state corresponds to the one extended over all basis states and has $I_2 = 1/N$.

[40] The relation $\Delta_e(e) = \frac{1}{\rho(e)\,\xi^d}$ is applicable only for the sparse matrices and not in case of the dense matrices. This can be explained as follows. Consider the matrix representation of an operator H in an arbitrary basis $|k\rangle$, $k = 1 \to N$, in which all off diagonals are of the same order (as in case of a BE). The matrix element, say, H_{kl}, can be written as $H_{kl} = \sum_{n=1}^{N} e_n\, U_{kn}\, U_{ln}^*$ with U_{kn} as the kth component of the eigenfunction U_n corresponding to the eigenvalue e_n of H. For cases where H is a random matrix, e_n are random variables too. Clearly, for H_{kl} to be of the same order for all basis pairs k, l for arbitrary $e_1, \ldots, e_N$, the correlation $U_{kn}U_{ln}^*$ should typically be of the same order (i.e., almost independent of k, l although it may depend on n). This requires a state U_n to typically have almost the same overlap with all basis states, thus implying an extended state in the volume L^d which in turn leads to $\Delta_e(e) = \frac{1}{\rho(e)\,L^d} = \frac{1}{R_1}$.